SCUOLA DOTTORALE IN BIOLOGIA MOLECOLARE CELLULARE E AMBIENTALE

XXXI CICLO

EVALUATION OF DNA DAMAGE IN MYOTONIC DYSTROPHY CELLS AFTER TREATMENT WITH DIFFERENT GENOTOXIC AGENTS

VALUTAZIONE DEL DANNO AL DNA INDOTTO DA DIFFERENTI AGENTI GENOTOSSICI IN CELLULE DI DISTROFIA MIOTONICA 1

PhD Student:
Sabrina Turturro

Tutor:
Prof.ssa Antonella Sgura

Coordinator
Prof. Paolo Mariottini

INDEX

ABBREVIATIONS 4
1. SUMMARY 6
2. RIASSUNTO 9
3. INTRODUCTION 11
3.1 Myotonic Dystrophies (DM): clinical features 12
3.1.1 DM1 molecular genetics 13
3.1.2 Oxidative stress in DM1 17
3.1.3 Premature aging in DM1 19
3.2 Chromosome instability (CIN) 23
3.2.1 Chromosome aberrations 24
3.2.2 Abnormal nuclear morphologies (ANMs) 26
3.2.3 Chromosome instability and telomeres 28
3.3 Oxidative stress (OS) 29
3.3.1 Oxidative stress and DNA damage 29
3.3.2 Oxidative stress and telomeres 30
4. AIM 34
5. RESULTS 36
5.1 DM1 cells $(CTG)_n$ repeat expansion size characterization 36
5.2 Mismatch repair (MMR) and Base Excision Repair (BER) systems are lower expressed in DM1 fibroblast respect to healthy control cells 38
5.3 X-ray induces a similar increase of aberration frequencies in both DM1 and WT 39
5.4 Oxidative stress induces oxidative base damage that does not persist 24h after treatment both in WT and DM1 cells 41
5.5 DDR response analysis 43
5.6 Abnormal nuclear morphology (ANMs) induction as a measure of chromosome instability induced by oxidative stress 44

5.8 Oxidative stress induces a decrease in cell growth rate correlated to an increase of senescence both in DM1 and WT cells 49

6. DICUSSION 53
7. CONCLUSION 57
8. BIBLIOGRAPHY 58
9. MATERIALS AND METHODS 69
Cell and culture conditions 69
PCR and fragment-length analysis 69
Triplet-repeat Primed (TP)-PCR 69
Southern blotting of long-range PCR-products 70
TaqMan Real-time qPCR 70
Irradiation Procedure 71
Collection of chromosome spreads 71
Multicolor-Fluorescence "in situ" Hybridisation Analysis (M-FISH) 72
H_2O_2 treatment 73
Standard and FPG-modified alkaline comet assay 73
SyBR Green Real-time qPCR 74
Cytokinesis-block micronucleus assay 75
Abnormal Nuclear Morphologies (ANMs) scoring criteria 75
Quantitative-Fluorescence "in situ" Hybridisation Analysis (Q-FISH) 75
Co-immunofluorescence 76
Growth rate analysis 77
Senescence beta-galactosidase Staining 77
Data analysis 77

ABBREVIATIONS

53BP1: *53 Binding Protein 1*
8-oxoG: 8-oxoguanine
ANMs: *Abnormal Nuclear Morphologies*
APE1: *apurinic/apyrimidinic endonuclease 1*
BER: *Base Excision Repair System*
BFB: *Breakage-Fusion-Bridge*
BN: *Binucleated cell*
CIN: *Chromosome Instability*
DDR: *DNA Damage Response*
DM: *Myotonic Dystrophy*
DM1: *Myotonic Dystrophy type 1*
DM2: *Myotonic Dystrophy type2*
DMPK: *Dystrophia Myotonica Protein Kinase gene*
DNA-PK: *DNA-dependent protein kinase*
DSBs: *Double-Strand Breaks*
DSBs: *Double-Strand Breaks*
ES: Error Standard
FPG: *Formamidopirymidine DNA glycosylase*
GPX: *Glutathione Peroxidase*
GSH: *Reduced Glutathione*
GST: *glutathione S-transferase*
H_2O_2: *Hydrogen Peroxide*
hESCs: *human Embryonic Stem Cells*
HR: *Homologous Recombination*
IR: *Ionizing Radiation*
LPO: Lipid Peroxidase
MDA: *Malonilaldheyde*
M-FISH: *multicolor FISH*
MLH1: *MutL homolog 1*
MLH3: *mutL homolog 3*
MMR: *Mismatch Repair System*
MN: *Micronuclei*
MSH2: *mutS homolog 2*
MSH3: *mutS homolog 3*
NBUDs: *Nuclear Buds*
NHEJ: *Non-Homologous End Joining*
NPBs: *Nucleoplasmic Bridges*

OGG1: *8-oxoG DNA Glycosylase 1*
OS: *oxidative stress*
PMS2: *PMS1 homolog 2*
qFISH: *quantitative FISH*
ROS: *Reactive Oxygen Species*
RT: *room temperature*
SD: Standard Deviation
SOD: *Superoxide Dismutase*
SSBs: *Single-Strand Breaks*
TAS: *Total Antioxidant Status*
TIFs: *Telomere-dysfunction induced foci*
T-loop: *Telomeric loop*
TP-PCR: *Triplet-repeat Primed PCR*
TRF1: *Repeat-Binding Factor 1*
TRF2: *Repeat-Binding Factor 2*
WT: *Healthy control cells*
ZNFP9: *Zinc finger Protein 9 gene*
γH2AX: *phosphorylation of H2AX*

1. SUMMARY

Myotonic Dystrophy type 1 (DM1) is a multisystemic disease caused by an unstable trinucleotide (CTG) repeat motif expansion in the 3' untranslated region (UTR) of the Dystrophia Myotonica Protein Kinase (DMPK) gene, located on chromosome 19q13.3 (1-3). It has a frequency of 1 of 8000 individuals worldwide (2, 3, 6, 7). The length of $(CTG)_n$ repeats is inversely correlated with the age of onset of the disease and consequently with its severity (1-3, 8, 12, 13). DM1 disease is characterized by somatic mosaicism: the existence of cells with different expansion length within an organism. In fact, some tissues and cell types possess a higher tendency to extend these tandem repeats sequences and the longest tandem repeats have been found in severely affected tissues (2, 8, 12-15). Furthermore, DM1 has been proposed as a disease due to an increased susceptibility to oxidative stress (OS) with high level of free radicals and reduced cellular antioxidant activity and premature aging (2, 42, 43) and there are evidences that the susceptibility to OS is $(CTG)_n$ repeats number-dependent (57, 58).

Mismatch Repair (MMR) protein complex in particular MSH2, MSH3 and PMS2, and Base Excision Repair (BER) components such us OGG1 can interact and cooperate to increase trinucleotide repeats instability (29, 33, 41, 47, 49). In particular MMR pathway is involved in repairing secondary structure acquired by DNA, while BER pathway is involved in repairing modified basis such as 8-oxoGuanine (8-oxoG) prevalently induced by OS.

A direct prove of the implication of MMR component in trinucleotide expansion in DM1 has been demonstrated by Seriola et al., (33) who for the first time demonstrated the down-regulation of MMR components in differentiated DM1 human Embryonic Stem Cells (hESCs) correlated to triplet expansion stabilization (33). On the other hand, there are no direct evidence about an involvement of BER pathway in this disease.

Starting from this knowledge, we wanted to understand the main mechanisms involved in DNA damage response (DDR) in this disease.

In order to reach this purpose we first characterized our fibroblasts. After having quantified the $(CTG)_n$ expansion size we evaluated the gene expression profile of MMR and BER mechanism components: we found them both down-regulated respect to the WT fibroblasts. In

order to study the effects of the expression profile analyzed and then the repair systems, we tried to evaluate the response to two different genotoxic agents: X-rays and H_2O_2.

We evaluated different markers of chromosome instability (CIN), and we found a higher basal level for all of them in DM1 cells respect to the WT, according to the lower level of MMR and BER gene expression they have. Furthermore, X-rays treatment (2 Gy) allowed us to evaluate Non-Homologous End Joining (NHEJ) and Homologous Recombination (HR) working by the analysis of breaks, fragments and translocations. After 24 hrs from treatment the analysis of karyotype of DM1 and WT cells allowed us to exclude a possible misregulation of both HR and NHEJ, in fact the increase of chromosome aberration was similar in DM1 and WT fibroblasts, for all the targets evaluated.

The treatment with H_2O_2 (200 µM, 1 hr) allowed us to evaluate the activation of both MMR and BER pathways. By FPG-modified comet assay we demonstrated that, both in DM1 both in WT, genomic DNA damage induced by OS, in particular 8-oxoG, were completely repaired within 24 hrs, suggesting a similar trend of repair kinetic in our samples, although oxidative DNA damage induced in DM1 cells was higher. These data are correlated with the gene expression profile in both our samples that showed an activation of both pathways already at 45 mins of treatment. Surprisingly, the analysis of Abnormal Nuclear Morphologies (ANMs) showed a greater increase of all the markers analyzed (micronuclei, MN; nucleoplasmic bridge, NPBs and nuclear Buds, NBUDs) in DM1 fibroblasts respect to WT at 48 hrs (especially in DM cells) persisting up to 72 hrs.

Recently, some authors have demonstrated that ANMs could be associated also with telomere dysfunction (77, 91). In fact, Pampalona et al., (91) have proposed that in particular the NPBs derive from end-to-end fusions, affecting chromosomes with critically short telomeres that leads to chromosome-end-fusions, visible as NPBs in interphase. For this reason, we investigated telomere length in DM1 and WT fibroblasts. As expected (59, 68), DM1 fibroblasts showed shorter telomeres respect to WT fibroblasts. After H_2O_2 (200 µM, 1 hr) treatment, WT and DM1 fibroblasts showed a telomere length reduction, as expected (77). In order to understand if DM1 telomeres are dysfunctional we evaluated the frequency of co-localization between TRF1, a shelterin complex protein, and γH2AX, a marker of double strand breaks (DSBs). In fact, in somatic cells telomeres that

reach the critical length could be recognized as DSBs and activate the DDR pathway, leading to senescence (65). The analysis of telomere dysfunction-induced foci (TIFs) showed a significant increase of γH2AX TIFs 48 hrs after treatment for DM1 fibroblasts, while a lower increase in WT ones. These results well correlate with the increased number of NPBs we found at 48 hrs from treatment and with the consequent increase of MN and NBUDs at 72hrs due to the NPBs breaks. The short telomere length we found in DM1 untreated fibroblasts also justify the higher basal levels of NPBs in these cells. All these data strongly correlate with the finding reported in Coluzzi et al, 2014 (77), in which in MRC-5 fibroblasts treated with H_2O_2 an increase of γH2AX TIFs was correlated with a telomere shortening and with an increase of NPBs at 48 hrs that give rise to MN and NBUDs at 72 hrs (77). As in our case, also in this case the genomic FPG-comet assay showed a total rescue of the oxidative DNA damage within 24 hrs, but the FPG-sensitive base lesions within telomeric DNA revealed a significant persistence of oxidative DNA damage at telomere 24 hrs from treatment, suggesting that oxidative DNA damage repair may be less effective in telomeres (77).
This allow us to hypothesize that also in our cells this phenomenon could occur and that at telomere level probably the oxidative damage could persist inducing the telomere dysfunction and the related ANMs observed (in DM1 more than in WT).
Because of the role of telomeres in cellular growth and senescence, these two end-points were studied. We observed a strong proliferative arrest that persist until 168 hrs for both WT and DM samples. These results were strongly supported by the senescence β-galactosidase staining that revealed a percentage of senescent cells from 50 to 65%. Therefore, considering the greater damage observed in DM cells but a similar trend of cellular growth and senescence, this leads us to hypothesize that probably DM1 fibroblasts could have a less regulated cell cycle checkpoint that allow a DNA damage that normal cells would not tolerate. On the other hand, considering the high rate of senescent cells, it could be interesting to analyze the destiny of these cells both in DM1 and WT at longer time, in order to evaluate if they are able to recover the proliferative block or if they die.

2. RIASSUNTO

La Distrofia Miotonica di tipo 1 (DM1) è una malattia multisistemica causata da una espansione di triplette (CTG) instabile localizzata nella regione 3'UTR del gene Distrofia Miotonica Proteina Chinasi (DMPK), localizzato sul cromosoma 19q13.3 (1-3). Questa malattia ha una frequenza di 1 su 8000 individui nel mondo (2, 3, 6, 7). La lunghezza dell'espansione $(CTG)_n$ è inversamente proporzionale all'età di esordio della malattia mentre è direttamente alla gravità dei sintomi (1-3, 8, 12, 13). La DM1 è caratterizzata da mosaicismo somatico: la coesistenza di cellule con espansioni di diversa lunghezza. Infatti alcuni tipi cellulari e tessuti hanno una maggiore predisposizione ad estendere le ripetizioni in tandem e espansioni più lunghe sono ritrovate nei tessuti maggiormente affetti (2,8,12,15). Inoltre, la DM1 presenta una elevata suscettibilità allo stress ossidativo (OS) con elevati livelli di radicali liberi e ridotta attività di antiossidanti; è una malattia da invecchiamento precoce (2, 42,4 3) e ci sono evidenze che la suscettibilità al OS sia direttamente proporzionale alla lunghezza delle espansioni (57, 58). Proteine del Mismatch Repair (MMR), in particolare MSH2, MSH3 e PMS2, e del Base Excision Repair (BER), come ad esempio OGG1, possono interagire e cooperare per aumentare l'instabilità delle espansioni (29, 33, 41, 47, 49). In particolare il MMR è coinvolto nella riparazione delle strutture secondarie acquisite dal DNA, mentre il BER nella riparazione delle basi modificate come la 8-oxoGuanina (8-oxoG) prevalentemente indotta dallo OS. Una prova diretta del coinvolgimento del MMR nell'espansione delle triplette nella DM1 è stata data da Seriola et al. (33), che per primi hanno dimostrato una down-regolazione dei componenti del MMR in cellule differenziate da cellule staminali embrionali umane (hESCs) di DM1 correlata alla stabilizzazione dell'espansione (33). D'altro canto, non ci sono evidenze dirette del coinvolgimento del BER in questa malattia. Partendo da queste conoscenze, abbiamo cercato di comprendere quali fossero i principali meccanismi coinvolti nella risposta al danno al DNA (DDR) in questa malattia. Per prima cosa abbiamo caratterizzato fibroblasti ottenuti da biopsia cutanea di pazienti di DM1. Dopo aver quantificato la lunghezza dell'espansione abbiamo valutato i livelli basali di espressione genica sia del MMR che del BER, trovandoli entrambi down-regolati rispetto ai fibroblasti WT di controllo. Per capire gli effetti di questo profilo di espressione genica e le risposte

dei sistemi di riparazione, abbiamo valutato la risposta di queste cellule a due agenti genotossici: raggi-X e H_2O_2.Abbiamo valutato diversi markers di instabilità cromosomica (CIN), e per tutti abbiamo trovato un più alto livello basale nelle cellule DM1 rispetto alle WT, probabilmente dovuto al loro minore livello di espressione genica di MMR e BER. Il trattamento con raggi-X (2 Gy) ci ha permesso di valutare il funzionamento di Non-Homologous End Joining (NHEJ) e Homologous Recombination (HR) attraverso l'analisi di rotture, frammenti e traslocazioni. A 24 hrs dal trattamento, l'analisi del cariotipo dei nostri campioni ci ha permesso di escludere una possibile deregolazione di NHEJ e HR, infatti per tutti i target analizzati cellule DM1 e WT mostravano lo stesso incremento. Il trattamento con H_2O_2 (200µM, 1 hr), invece, ci ha permesso di testare MMR e BER. Mediante il FPG-comet abbiamo dimostrato che il danno genomico indotto dallo OS, e in particolar l'8-oxoG, era completamente riparato entro le 24 hrs sia nelle cellule DM1 che WT, suggerendo una simile cinetica di riparazione, nonostante un maggiore livello di danno ossidativo indotto nelle cellule DM1. L'analisi del profilo di espressione genica ha mostrato in entrambi i campioni una attivazione di MMR e BER già a 45 mins di trattamento. Sorprendentemente, l'analisi delle anomalie nucleari (ANMs) ha rivelato un maggiore aumento di tutti i target analizzati (micronuclei, MN; ponti nucleoplasmici, NPBs, Bud nucleari, NBUDs) nelle cellule DM1 rispetto alle WT a 48 hrs dal trattamento. Questo danno persisteva fino a 72 hrs. Recentemente, alcuni autori hanno dimostrato che le ANMs potrebbero essere associate a disfunzione telomerica (77, 91). Infatti, Pamplaona et al., (91) hanno proposto che in particolare i NPBs, possano derivare da fusioni terminali di cromosomi con telomeri molto corti, visibili come NPBs in interfase. Per questo motivo abbiamo valutato le lunghezze telomeriche dei nostri campioni. Come atteso (59, 68), i fibroblasti DM1 avevano telomeri più corti rispetto a quelli WT. A 48 hrs dal trattamento, come atteso (77), entrambi mostravano una riduzione delle lunghezze telomeriche. Quindi, per capire se i telomeri dei fibroblasti DM1 fossero disfunzionali, abbiamo valutato la frequenza di co-localizzazione tra γH2AX, un marker di rotture a doppio filamento (DSBs), e TRF1, una proteina del complesso shelterin. Infatti, nelle cellule somatiche telomeri troppo corti e non in grado di ripiegarsi a formare il T-loop possono essere riconosciuti come DSBs e attivare la DDR, conducendo alla senescenza cellulare (65). L'analisi dei foci indotti da telomeri

disfunzionali (TIFs) ha mostrato un significativo aumento di TIFs di γH2AX a 48 hrs dal trattamento nelle cellule DM1, e minore nelle cellule WT. Questi risultati correlano molto bene con l'aumento di NPBs trovato a 48 hrs dal trattamento che sfocia in un aumento di MN e NBUDs a 72 hrs dovuto alla rottura dei NPBs. I telomeri corti che abbiamo trovato nelle cellule DM1 non trattate giustificano anche gli alti livelli basali di NPBs. Tutti questi dati correlano fortemente con quanto dimostrato da Coluzzi et al., (77): fibroblasti MRC-5 trattati con H_2O_2 mostravano un aumento di TIFs di γH2AX correlato a un accorciamento telomerico e a una induzione di NPBs a 48 hrs che sfociava in un aumento di MN e NBUDs a 72 hrs dal trattamento (77). Come nel nostro caso, anche nelle MRC-5 il FPG-comet genomico mostrava una totale riparazione del danno ossidativo entro 24 hrs dal trattamento, ma un saggio in grado di misurare il livello di 8-OxoG specificatamente nelle regioni telomeriche dimostrava una persistenza significativa del danno ossidativo a 24 hrs, suggerendo una sua minore riparazione al telomero (77). Questo ci permette di ipotizzare che anche nelle nostre cellule possa essersi verificato lo stesso fenomeno, dati gli alti livelli di TIFs e di ANMs (più nelle cellule DM1 che WT). Dato l'importante ruolo del telomero nelle crescita cellulare e nella senescenza, abbiamo valutato questi due eventi. Abbiamo osservato un arresto della crescita cellulare a partire da 48 fino a 168 hrs post-trattamento correlato a un aumento della senescenza dal 50 al 65%. Dunque, l'elevato danno riscontrato nelle cellule di DM1, ma il simile trend di crescita e di senescenza rispetto alle cellule WT ci permettono di ipotizzare che nelle cellule DM1 potrebbe essere alterato un checkpoint del ciclo cellulare che permetta loro di tollerare livelli di danno che cellule sane non tollererebbero. D'altro canto, considerando l'elevato livello di cellule senescenti, potrebbe essere interessante analizzare il destino sia delle cellule DM1 che WT a tempi più lunghi, per valutare se siano in grado di recuperare da questo blocco proliferativo o se il loro destino sia la morte.

3. INTRODUCTION

3.1 Myotonic Dystrophies (DM): clinical features

Myotonic Dystrophy (dystrophia myotonica, or DM) is one of the most common lethal monogenic disorders in populations of European descent (1-3). It is a multisystemic disorder linked to two different genetic loci, and for this reason it is known as type 1 and type 2 (1-3). Myotonic Dystrophy type 1 (DM1), also known as Steinert's disease (OMIM: 160900) is caused by an unstable trinucleotide (CTG) repeat motif expansion in the 3' untranslated region (UTR) of the *Dystrophia Myotonica Protein Kinase (DMPK)* gene, located on chromosome 19q13.3 (1-3) (fig.1). A second form of DM, discovered about a decade after DM1, is Myotonic Dystrophy type 2 (DM2) (OMIM: 602668), initially named as Proximal Myotonic Myopathy due to the greater weakness of proximal as compared to distal muscles in DM1 (1, 4, 5). DM2 is caused by a tetranucleotide (CCTG) expansion in intron 1 of the *Zinc Finger Protein 9 (ZNF9 or CNBP)* gene on chromosome 3q21 (1, 2, 4) (fig.1).

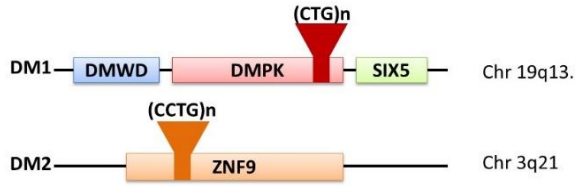

DMPK: *Dystrophia Myotonica Protein Kinase - 5-38 repeats healthy people, between 50 and several thousand affected*

ZNF9 *(CNBP): Zing Finger Protein 9 - <30 repeats healthy people, between 50 and 11000 patients*

Figure 1 Representation of the DM-causing genes, the location of the tandem repeats and their neighboring genes. Modified by (2).

DM1 is one of the most prevalent forms of muscular dystrophy with a frequency of 1 of 8000 individuals worldwide (2, 3, 6, 7). Otherwise, the frequency of DM2 is uncertain, but most recent reports suggests that its incidence could be as high as DM1 (1, 3, 8).

Both DM1 and DM2 share a repeat expansion in noncoding regions of genes (DMPK and ZNF9) that are expressed especially in tissues affected by this disease.

Since in both genes the repeat expansions is located in transcribed but untranslated regions the mutant RNA might have a significant role in

the disease process (1-3): aberrant RNA are accumulated in the nucleus and act in trans on the splicing and expression levels of many other genes (1, 3, 9, 10). However, a key difference between these two diseases is that only DM1 locus presents a congenital form of this disorder, while DM2 no (1, 11).
The previously described nucleotide expansions lead to the progressive degeneration of several tissues and organs, which is more prominent in DM1 and milder in DM2 patients (2) (fig.2).

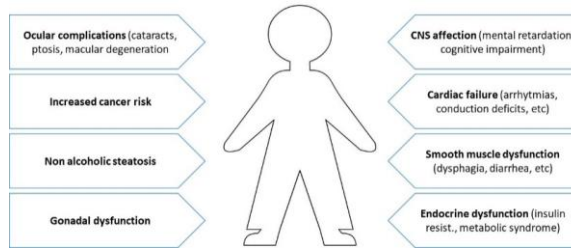

Figure 2 Summary of main symptoms affecting DM patients, which constitute the multisystem affectivity found on them. Modified by (2).

DM patients may suffer a broad variety of symptoms affecting the three muscles type: cardiac, skeletal and smooth muscles. Although the initial pattern of muscles weakness is notably different between DM1 and DM2 (distal vs proximal), the muscles biopsies show a similar histology of central nucleation and increased fibre sizes, which is a feature of constantly regenerating muscles with immature fibres (1-3).

3.1.1 DM1 molecular genetics

In patient with DM1, $(CTG)_n$ expansion range from 51 repeats to several thousand, while healthy individuals carry 5-37 repeats (3, 12). Repeats length of 38-50 are considered premutation alleles, whereas 51-100 repeats are considered protomutation, both of which show increased instability towards expansion (3, 12). Carriers of premutation or protomutation present no or few mild symptoms, such as cataract (1, 2, 8). Patients with adult-onset DM1 carry more than 100 repeats, and those with congenital DM1 have more than 1000 repeats: the length of $(CTG)_n$ repeats is inversely correlated with the

age of onset of the disease and consequently with its severity (1-3, 8, 12, 13). DM1 disease is characterized by *somatic mosaicism*: the existence of cells with different expansion length within an organism. In fact some tissues and cell types possess a higher tendency to extend these tandem repeats sequences and the longest tandem repeats have been found in severely affected tissues (2, 8, 12-15). Cells with longer expansion length are more prone to expand their repetitions than cells with shorter repeated sequences (2, 3, 16-20). In addition to somatic cells, also germline cells are prone to genomic instability and thus accumulate repeats expansion: DM1 repeat expansion tends to increase its size after each cell cycle, leading to *anticipation*, which refers to the increase of severity and decrease in the age of onset in each generation of affected families (2, 3, 6, 12, 19, 20). Table 1 shows a summary of repeat range, penetrance, age of onset and phenotypes (21).

Table 1 ***Summary of repeat range, penetrance, age onset and phenotypes (21).***

Phenotype	Most prominent clinical symptoms	Repeat range	Age of Onset	Life Span	Penetrance and Anticipation (Yes/No)
Pre-mutation	None	38–49	-	Normal	At increased risk of penetrance Uncertain
Late-onset DM1	Cataracts, hypersomnia, myotonia	100–600	>40 years	Normal	Full Penetrance Yes
Adult DM1	Myotonia, cardiac arrhythmias, hypersomnia, gastrointestinal difficulties, muscle weakness and wasting, cataracts, male hypogonadism, insulin resistance, cognitive challenges, left ventricular dysfunctions	250–750	20–40 years	Shortened	Full Penetrance Yes
Juvenile DM1	Similar symptoms as adult DM1 but more severe	400–800	10–20 years	Shortened	Full Penetrance Yes
Infantile DM1	Similar symptoms as congenital DM1 but less severe	500–1100	1 mo. – 10 years	Shortened	Full Penetrance Yes
Congenital DM1	Developmental defects, hypotonia, respiratory insufficiency, cardiac defects, severe cognitive challenges, facial dysmorphism, dysphagia	750–1400	Birth	At increased risk of infant mortality or shortened	Full Penetrance Yes

Previous studies suggest that generally triplet-repeat expansion occurs not only during DNA replication (22-25) but also during DNA repair (18, 22, 25-29). DNA tandem repeats acquire secondary structure, usually forming hairpins, loops, triplet helices, and G-quadruplex (19, 24, 30) resulting as substrate for DNA damage response (DDR) (18, 19, 23-25, 28, 29), in particular for Mismatch Repair System (MMR).

MMR protein complex[1], in particular MSH2, MSH3 and PMS2[2], are involved in trinucleotide repeats instability (19, 22, 28, 29, 31-34). DM1 Knockdown mouse models for *Msh2* and *Msh3* show stabilization or contraction of the trinucleotide expansion (22, 33, 35-37); PMS2 is known to be an enhancer of somatic mosaicism of trinucleotide repeats (33, 38), moreover the concentration of the levels of MSH3 in DM1 mice determines the size of $(CTG)_n$ expansion (33, 37). Thus in presence or in absence of MSH2 and MSH3, large expanded CTG repeats show respectively the 90% expansion/contraction of their length (19, 22, 33, 35-37, 39). It seems that the hairpin structure of the trinucleotide-repeat expansion forms a unique DNA junction that traps MutSβ (complex by MSH2 and MSH3) responsible to target small insertion/delection, on the template (40, 41) hampering its function and diverting the hairpin structure correction to other DNA repair systems which will give rise to trinucleotide expansion (41). Moreover, at higher MutSβ complex concentration the proper slipped-CTG repair is hampered and, likely error-prone, $(CTG)_n$ repeats are expanded (32, 33). A direct prove of the implication of MMR component in trinucleotide expansion in DM1 has been demonstrated by Seriola et al. (33). They have demonstrated that while in human Embryonic Stem Cells (hESCs) there is a higher DNA instability and MMR components are largely expressed, upon differentiation these cells dramatically reduce the MMR component expression in concomitant with the stabilization of the expansions size (33).

Furthermore, DM1 has been proposed as a disease due to premature aging and free radical production (2, 42, 43) (see paragraph 3.1.2). In fact recent studies suggest that $(CTG)_n$ triplet expansion occurs also during the repair of DNA lesions induced by oxidative stress (OS) (19,

[1] MMR machinery corrects not only errors that escaped the DNA polymerase proofreading function, but also recognize mispaired bases and branched DNAs formed during recombination as well as chemically modified bases in DNA. It is composed of various interacting proteins: MSH2, MSH3, MSH6, MLH1, MLH3, PMS1, PMS2 (19, 20).

[2] MSH2 and MSH6 form MutSα that preferentially targets mismatched bases; MSH2 and MSH3 form MutSβ that preferentially targets small insertion/deletion; MLH1 and PMS2 form MutLα which is a esonuclease responsible to cleave DNA of the lesioned strand, this action could also be performed by MutLβ complex of MLH1 and PMS1, and MutLγ complex of MLH1 and MLH3 (19, 20).

22, 24, 29, 44, 45), preferentially repaired by Base Excision Repair[3] (BER) mechanism (46). Guanine residues within $(CTG)_n$ repeats are particularly susceptible to oxidative DNA damage, resulting in 8-oxoGuanine (8-oxoG) lesions (19, 22, 29). 8-oxoG may induce formation of protoexpansion intermediates through strand slippage during DNA BER repairing: the action of 8-oxoG DNA Glycosylase 1 (OGG1) generates an abasic site, which in turn is substrate for apurinic/apyrimidinic endonuclease 1 (APE1) (19, 22, 29, 41). The resulting strand incision can then form a stable hairpin structure (29, 47, 48) that could form complex with MutSβ, leading to trinucleotide expansion (19, 22, 24, 29). So it seems that MMR proteins may increase the likelihood that oxidative damage will occur by stabilizing secondary structures that are sensitive to such damage (29, 41, 47-49). It could also be that MMR acts later than BER pathway by stabilizing the hairpin structure generated by strand-slippage thus increasing the likelihood that priming will occur from the slipped position during repair synthesis (29, 33, 41, 47-49) (fig.3).

While for MMR components we have a direct prove of their involvement in triplet expansion in DM1 (33), for BER components we have not any direct evidence in this disease, only the information that the high OS induces BER that trigger the MMR activation and thus the triplet expansion (19, 29, 41). On the other hand, mechanisms involved in DNA Double Strand Breaks (DSBs) repair aren't involved in repeat expansion in mammalian systems (41). In fact, neither the loss of RAD52 nor the loss of RAD54, proteins both involved in Homologous Recombination (HR) repair system, affected expansion size (36, 41). On the other side, RAD52 also cooperates with OGG1 in the repair of oxidative stress induced DNA damage, so this protein could have a role in trinucleotide-repeat expansion independently of its role in HR (41, 50). In addition, the absence of DNA-dependent protein kinase (DNA-PK), involved in Non-Homologous End Joining (NHEJ), had no effect on the trinucleotide-repeat expansion frequency (36, 41).

[3] BER has evolved to protect cells from the deleterious effect of endogenous DNA damage induced by hydrolysis, reactive oxygen species (ROS) and other intracellular metabolites that modify DNA base structure (46).

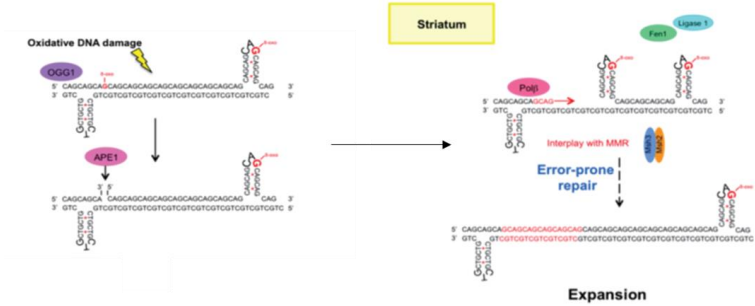

Figure 3 MMR and BER crosstalk. Modified by (48).
Base excision repair (BER)-induced CAG repeat expansion is tissue-dependent. Oxidative DNA lesions, including 8-oxoG lesions, occur stochastically at trinucleotide CAG repeats and are processed by the BER pathway. A DNA glycosylase (e.g., Ogg1) and Ape1 initiate repair. In the striatum, where Fen1 and Lig1 proteins are reduced, repair of the DNA lesion at CAG repeats is error-prone. The flappy structure is not efficiently processed, which ultimately leads to repeat expansion probably interacting with mismatch repair (MMR).

3.1.2 Oxidative stress in DM1

DM1 has been proposed as a disease due to premature aging and free radical production (2, 42, 43). In living organisms, there is an intricate balance between production and destruction of Reacting Oxidative Species (ROS) (51). Excess ROS reacts with a wide range of biomolecules such us DNA, lipids, and proteins (51-54), damages cell structure and is involved in the aging processes (51, 55, 56). Increased levels of ROS/free radicals and lipid peroxide levels and the antioxidant system have been investigated in DM1, supporting a possible role of oxidative stress in pathogenesis (42, 43, 51). Further evidences have showed an increased susceptibility to OS in cells with expanded $(CTG)_n$ repeats and that this susceptibility is $(CTG)_n$ repeats number-dependent (57, 58).

DM1 patients show a significant increase of Malonilaldheyde[4] (MDA), Superoxide Dismutase (SOD), and Total Antioxidant Status (TAS) levels (42, 43, 51) and Glutathione peroxidase (GPX), glutathione S-transferase (GST) and Reduced Glutathione[5] (GSH) reduction respect to healthy control (51), supporting the hypothesis that oxidative damage phenomenon is present in DM1 cells and may contribute to DM1 disease progression (42, 43, 51, 57, 58). Figure 4 shows how these enzymes act in OS pathway.

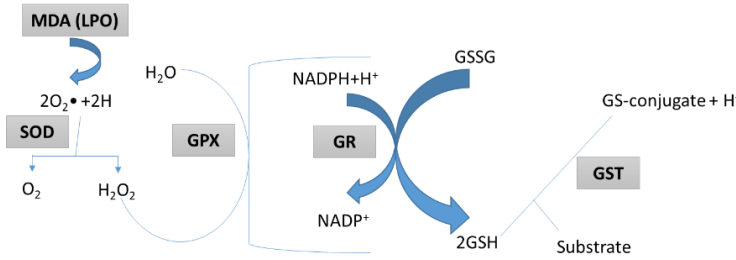

Figure 4 Schematic summary of the minisystem of antioxidation detoxification and repair. *Modified by (51).*
MDA increase the concentration of reactive oxygen species and peroxide. Two superoxide anions ($O_2\bullet$) are reduced by SOD to form molecular oxygen and hydrogen peroxide (H_2O_2), then H_2O_2 is reduced by GPX by oxidation of two molecules of glutathione (GSH), forming glutathione disulfide (GSSG) that subsequently can be reduced by Glutathione Reductase (GR) under consumption of NADPH. GST catalyzes the conjugation of glutathione with other biomolecules.

The increased levels of MDA and decreased levels of antioxidant enzymes GPX, GST and GSH involved in higher oxygen free radicals production lead cells to undergo stress condition: thus the increase of

[4] Is the principal and most studied final product of polyunsaturated fatty acid peroxidation and the greater enhancement of lipid peroxidase (LPO) in DM1 patient may be due to the excess formation of oxygen free radicals and peroxides that inactive several enzymes important in muscular energy production and aminoacid metabolism (42, 43, 51).
[5] With his thiol group is a potent reducing agent and detoxifies a variety of electro proton compounds and peroxidases via catalysing GST and GPX. Glutathione remains intracellularly as an oxidized and reduced state and their critical balance is crucial for cell survival (42, 43, 51).

SOD and TAS activity may be compensatory in response to an increased OS (51).

3.1.3 Premature aging in DM1

The CTG mutation is very unstable and its amplification occurs both over generations and in somatic tissues: in fact it is possible to measure somatic instability in DM1 patients throughout their life with a gradual increase in the average of their repeats expansion (1-3, 14, 15, 59). It is known that the size of $(CTG)_n$ expansion increases progressively at each cellular division during the proliferative lifespan of DM1 *satellite cells*[6] indicating a replication-dependent somatic instability (2, 59, 60). It is also known that proliferative capacity of satellite cells is significantly decreased in congenital DM1 patients respect to age-matched healthy controls (2, 59, 60). The proliferative capacity of human satellite cells, like the majority of human diploid somatic cells, is limited by cellular senescence (2, 59, 60). One major mechanism involved in replicative senescence of human cells is the progressive shortening of their telomeres after each cell cycle (2, 59, 61). Telomeres are nucleoprotein structures organized into heterochromatin domain and located at the end of linear chromosomes, which primary role is to maintain chromosome and genome stability (61-64). In human, telomeric DNA consists of conserved, non-coding regions composed by tandem repeats of the G-rich exanucleotide $(TTAGGG)_n$ in vertebrate, which are typically 10-15 Kb (61-64). It is oriented 5' to 3' towards the end of the chromosome, ending in a fundamental 3' single-G-stranded overhang which length was species specific (61-64). The end of chromosomes ended in a large loop (t-loop_telomeric loop) generated by the invasion of the 3' overhang of single-stranded TTAGGG into the duplex telomeric tract, resulting in the displacement of the TTAGGG repeat strand (d-loop_displacement loop) at the loop-tail junction. The circular segment of the loop is composed by duplex DNA (61-64) (fig.5).

[6] Muscle progenitor cells (2).

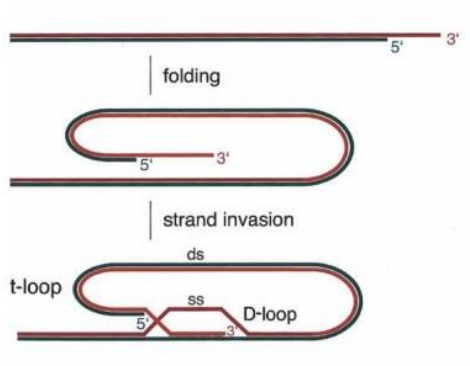

Figure 5 Telomeric loop formation.
The 3' single strand of telomeric DNA invades the duplex telomeric DNA forming firstly the displacement loop (d-loop) and finally the telomere loop (t-loop) (63)

Semi-conservative replication of eukaryotic DNA generates two different strands: the leading strand of DNA that is completely replicated, and the lagging strand that is not fully replicated. This difference is due to the inability of the conventional DNA polymerase to fully replicate the extreme 3' end of a DNA sequences in absence of a template strand (65, 66), leading to a loss of few bases of terminal genetic material at each cell division (fig. 6).

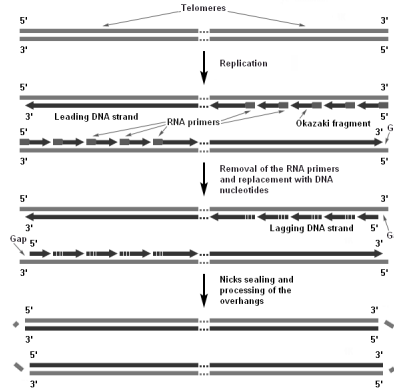

Figure 6 End-replication problem.
The removal of the last Okazaki fragment in the lagging strand leaves a gap of unreplicated DNA (66)

Once a critical short telomere length is reached, replicative senescence is triggered through a p53-dependent pathway (67).
The introduction of the catalytic subunit of the telomerase[7] (*hTERT*) gene into human fibroblast is normally sufficient to block telomere shortening and prevent replicative senescence in somatic cells, leading to their immortalization (68). However, this does not happen in case of satellite cells, where induced hTERT activity is not sufficient to confer immortality, indicating the existence of an alternative pathway responsible of their proliferative capacity regulation (59, 69). It is known that p16[8]-dependent pathway provokes proliferative arrest before telomeres reach their critical length, and its silencing in addition to hTERT expression results in immortalization of satellite cells, and other cell lines (59, 70, 71). p16 is upregulated in response to several telomere-independent stress mechanisms such as oxidative stress and DNA damages (72), but it is also known that it could be activated in response to telomere damage (73) and that its expression increase, in some progenitor cell lines during age, contributes to stem cell decline, senescence and aging (59, 74).
Large $(CTG)_n$ repeats expansion trigger *in vitro* a mechanism of premature senescence through a p16-dependent pathway (fig.7), which reduces significantly the proliferative capacity of DM1 muscle progenitor cells, and consequently their capacity to maintain the integrity and functional property of muscle fibres, contributing to their progressive atrophy (2, 59, 75).

[7] Telomerase is a reverse transcriptase enzyme that carries its own RNA molecule, which is used as a template when it elongates telomeres. It is active in normal stem cells and most cancer cells, but is normally absent from, or at very low levels in, most somatic cells (61).
[8] p16 is a tumor suppressor protein that is a cyclin-dependent kinase inhibitor and is essential in regulating the cell cycle (69).

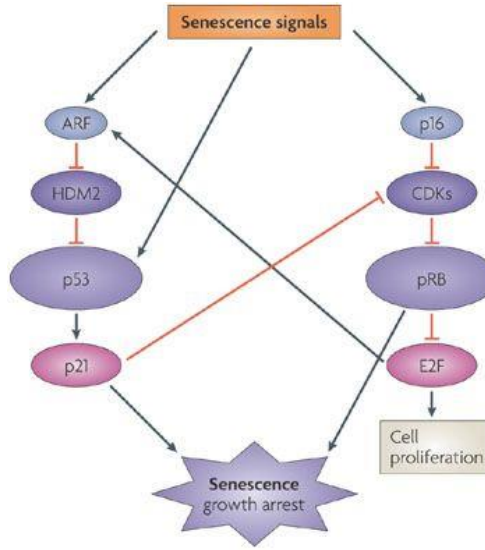

***Figure 7 Senescence-inducing signals** (74).*
Senescence signals that engage the p16–pRB pathway generally do so by inducing the expression of p16, a CDK inhibitor that prevents pRB phosphorylation and inactivation. pRB halts cell proliferation by suppressing the activity of E2F, a transcription factor that stimulates the expression of genes that are required for cell-cycle progression. E2F can also curtail proliferation by inducing ARF expression, which engages the p53 pathway. So there is reciprocal regulation between the p53 and p16–pRB pathways.

Measurements of telomeres length at the end of their lifespan indicated that DM1 cells had not yet exhausted their proliferative capacity, confirming their premature growth arrest independent from an excessive *in vivo* satellite cells turnover (2, 59, 75). Even if an alteration in telomere homeostasis, reflected by the accelerated telomere shortening, is measured in DM1 cells, the reintroduction of telomerase activity fails to extend their lifespan (59), suggesting a premature senescence independent from telomere. In fact DM1 satellite cells stop dividing with telomeres significantly longer than those of healthy cells (2, 59, 75), and the inactivation of p16 pathway in their satellite cells prevents their premature senescence and extend their lifespan (2, 59).

However, it still remains to understand if $(CTG)_n$ repeat expansion could interfere with telomere homeostasis. Trinucleotide expansion could adopt several secondary structures that disturb DNA metabolism and require the involvement of DNA repair systems (18, 19, 23-25, 28, 29). Because of proteins involved in telomere homeostasis regulation could also participate to the DNA damage response (DDR) (59, 76), it could be that the large $(CTG)_n$ expanded repeats may recruit telomeric/repair proteins leading to unstable chromosome ends, accelerating telomeres shortening (59). It is also known that telomere shortening is associated with higher OS levels (59, 77-79); the increased levels of free radicals and lipid peroxidation in DM1 patients (42, 43, 51), could contribute to telomere alteration in DM1 disease progression, considering also that the cellular susceptibility to OS is positively correlated with the number of $(CTG)_n$ repeats (58). According to this, Bigot et al have measured a 59% increase in the amount of telomeric DNA lost per division in DM1 cells respect to healthy control cells, in the same culture conditions (59).

3.2 Chromosome instability (CIN)

DNA is the molecule that contains all the genetic information responsible for development and function of cells, but also of the whole organism. Therefore, it is clear that the DNA damage, if not properly repaired, could have serious consequences on cellular stability and viability (80). CIN could be due to several processes as DNA damage (single - SSBs[9] and double strand breaks – DSBs)[10] (80-82) and chromosome malsegregation.

[9] The SSBs are characterized by a single break in one of the two strands of the DNA and they represent the most frequent damage that occur in the DNA (75).

[10] The DSBs probably represent the most dangerous lesions and are generated when the two complementary strands of the duplex DNA are broken, at the same time, at two different sites close to one another. In this case, the two DNA ends could not be juxtaposed; consequently, the two DNA ends dissociate from each other and the repair machinery cannot work correctly. This phenomenon gives the opportunity for inappropriate recombination with other sites in the genome leading to chromosome fusions (76).

3.2.1 Chromosome aberrations

Alteration in genetic materials through loss, gain or rearrangement of particular segments generate chromosome aberrations. Chromosome aberrations can be divided in two main categories: numerical and structural ones.

Numerical chromosome aberrations are alteration in the correct number of the chromosomes of the specie (euploidy). Numerical chromosome aberration can involve the alteration of a whole set of chromosomes (polyploidy) or the gain or loss of specific chromosomes (aneuploidy).

Variation in the number of chromosomes is mainly due to the abnormal segregation during mitosis or meiosis. In opposite to normal disjunction, that is responsible to guarantee the normal set of chromosomes to the daughter cells, malsegregation is the one of the causes of aneuploidy and it results deleterious for cells since it causes a displacement in the chromosomes set (80).

Structural aberrations of chromosome are due to a breakage and rearrangement of DNA (inversion, translocation, deletion, insertion, duplication) while the number of chromosomes remains unvaried (83). Structural chromosome aberrations can also be classified into "stable" or "unstable" originated by events of DBSs not repaired or incorrectly repaired.

In stable aberrations there is neither gain nor loss of DNA and they persist in the genome during the whole lifespan of the cells (83). Between these, there are (fig.8):

- inversion, when a segment of a chromosome is found to be oriented in reverse direction leading to an opposite order of the genes;
- translocation, when chromosome segment is integrated into a non-homologous chromosome; the transfer could take place in a different part of the same chromosome or in a different chromosome.

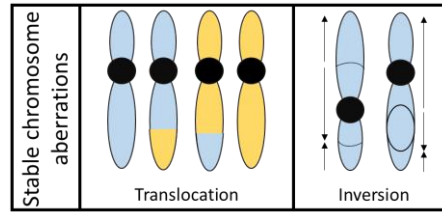

Figure 8 Stable chromosome aberrations.

Stable aberrations, without the loss of genetic information, are not recognized by the DNA damage machinery or by the apoptosis mechanisms; therefore they could be responsible for tumor development (84).

On the contrary, unstable aberrations are so defined because give rise to gain and/or loss of DNA and are prone to variability during the subsequent cell division (83). Briefly, we can include (fig.9):

- deletion: the loss of a chromosome fragment;
- duplication: the presence of an additional segment of chromosome;
- dicentric chromosome: a chromosome with two centromeres raised after the fusion of two different chromosomes. This fusion, among others, could be due to the telomere loss that originate sticky ends that can fuse each other. During mitosis, the two centromeres of this dicentric chromosome could be pulled to the opposite pole of the cell leading to a chromosome break.

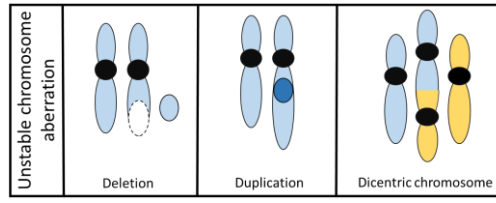

Figure 9 Unstable chromosome aberrations.

Unstable aberrations could change the normal state of the cell that can be eliminated by apoptosis (85).
Both stable and unstable chromosome aberrations could be detected blocking cells in metaphase, but CIN could be also evaluated in interphase nuclei by the study of biomarkers called Abnormal Nuclear Morphologies (ANMs), such us Micronuclei (MN), Nucleoplasmic Bridges (NPBs) and Nuclear Buds (NBUDs) (86).

3.2.2 Abnormal nuclear morphologies (ANMs)
Abnormal Nuclear Morphologies (ANMs) represented by Micronuclei (MN), Nuclear Buds (NBUDs) and Nucleoplasmic Bridges (NPBs) are biomarkers of CIN (87) (fig. 10). All of these biomarkers are observable in interphase nuclei only if cells were treated with cytochalasin B, a cytokinesis inhibitor that allow the formation of a binucleated cell (BN), cell with two daughter nuclei in the same cytoplasm, that allows to observe the ANMs, otherwise lost during the cell division (87).

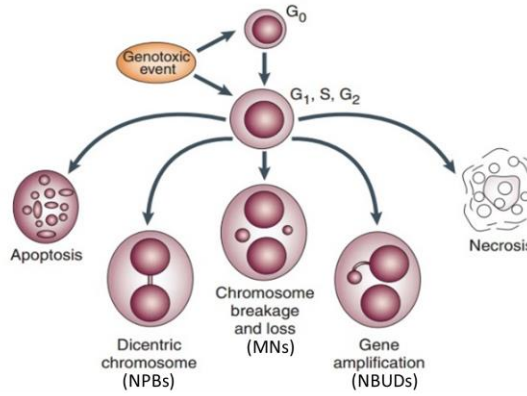

Figure 10 Possible fates of cultured cells after exposure to genotoxic agents (88).

MN derive from whole chromosome or chromosome fragments that hang back during anaphase and fail to be included in the daughter nuclei. They are similar to a daughter nucleus but with smaller size (87). MN that contain whole chromosome originate from defects in spindle assembly, mitotic checkpoints, kinetochore proteins assembly or for the failed attack to the spindle (89, 90). On the contrary, MN that contain chromosome fragments occur after a DSB that gives rise to an acentric fragment that escape from the spindle (87) (fig.11).

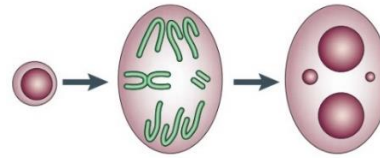

Figure 11 Origin of micronuclei. MN can originate both from acentric chromosomes and a whole chromosome (88).

NBUDs have the same morphology as a MN, even if they are still connected to one of the daughter nuclei by a slight stem of nucleoplasmic material. The NBUDs could eventually break away giving rise to a MN (87).
NPBs are nucleoplasmic bridges originating during anaphase when dicentric chromosomes are pulled to opposite poles of the cell (91) (fig.12). During the cytokinesis, the NPBs will break forming again two different sticky ends (*Breakage-Fusion-Bridge*-BFB cycles) and generating a high level of genomic instability within the cells (92). Another possibility is that the NPB breaks in two different sites giving rise to a MN; while if it breaks in only one site it can give rise to a NBUDs (93).

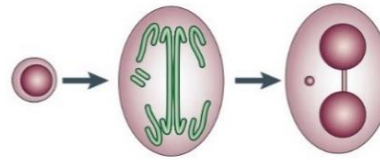

Figure 12 Origin of nucleoplasmic bridge. NPB is formed when the two centromeres of a dicentric chromosome are pulled to the opposite pole of the cell (88).

3.2.3 Chromosome instability and telomeres

It is known that telomeres that loose the t-loop can be recognized as DSBs (62, 94) and can determine chromosome instability through the BFB cycles (95). Recently, some authors have demonstrated that ANMs could be associated also with telomere dysfunction. In fact Pampalona et al., (91), by telomeric FISH in BN cells, have proposed that most of the abnormal nuclear morphologies, in particular the NPBs, derive from end-to-end fusions, affecting chromosomes with critically short telomeres (fig.13). In fact, the loss of the t-loop structure by telomere shortening damages the protection of the chromosome end and leads to chromosome-end-fusions, visible as NPBs in interphase. NPBs can break in one or two different sites giving rise respectively to the formation of NBUDs and MN suggesting a common origin of all these structures. This phenomenon validates the use of these abnormal nuclear morphologies as biomarkers also of telomere-dysfunction dependent chromosomal instability (91).

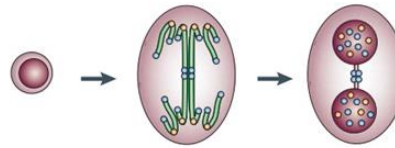

Figure 13 NPBs can originate from telomeric fusion. Blue spots represent telomeric probe, yellow spots the centromeric probe (88).

3.3 Oxidative stress (OS)

Oxidative stress represents an imbalance between the production of Reactive Oxygen Species (ROS) and the ability of the biological systems to readily detoxify the reactive intermediates or to repair the resulting damage.

3.3.1 Oxidative stress and DNA damage

Normal biological process and exogenous oxidative agents could both increase the levels of ROS within the cells. O_2 is involved in many chemical reactions important for cell viability. Normally molecular oxygen is not much reactive, but due to temperature, radiation, chemical agents or cellular metabolism, it can be transformed in ROS (96). These molecules are highly reactive and unstable (96) and could interact and damage different cellular components, such us proteins, lipids and DNA. Oxidative DNA damage constitutes the majority of DNA damage in human cells (52). ROS represent a source of oxidative stress due to the production of SSBs anywhere in the genome (97), directly or as an intermediate step in the repair of oxidative base modifications (98). If not repaired SSBs could became DSBs and lead to chromosome aberrations (80).

One form of DNA damage induced by oxidative stress is the modification of DNA bases such as 8-oxoG, thymine glycol, and 5-hydroxy-methyluracil. The 8-oxoG is recognized as typical biomarker of oxidative DNA damage (99). It can be repaired correctly by 8-oxoguanine glycosylase 1 (OGG1) and BER systems (100-103), or if not, it can induce single or double strand breaks and GC-AT mutation (101) (fig.14).

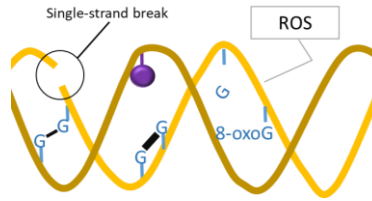

Figure 14 Principal DNA damages induced by ROS. Modified by (104).

3.3.2 Oxidative stress and telomeres

As known, in somatic cells, telomeres get shorter at each cell division (65). The rate of telomere shortening could be accelerated significantly by environmental agents, as well as radiation and chemical agents, that promote the gradual loss of sufficient repeated sequences necessary to maintain proper telomere structure (79, 105).

Literature data have demonstrated that oxidative stress can accelerate telomere shortening in *in vitro* replicating fibroblasts, through the induction of SSBs at telomeres (106). Because of the principal DNA damage induced by oxidative stress is 8-oxoG, the probability of the accumulation of this lesion within telomeres during oxidative stress is enhanced by the high incidence of guanine residues in these DNA sequences (107). Moreover the guanine expressed in sequences GG or GGG are more susceptible to oxidation than the single guanine (108), supporting the hypothesis that telomeric sequence is one of the first target of oxidative damage (109). Furthermore, the damage in heterochromatic region is less efficiently repaired compared to the rest of the genome. The presence of 8-oxoG leads to telomere shortening and alterations in telomere maintenance and function (65). In fact this lesion within telomeric DNA interferes with the replication fork at telomeres and aborted replication may lead to strand breaks and loss of telomeric repeats (79).

Moreover, this telomeric oxidative lesion may interfere directly with the recognition by telomeric repeat binding factor 1 and 2 proteins (TRF1 and TRF2)[11] to telomere repeats (110, 111), leading to telomere dysfunction (fig.15).

[11] Telomeric DNA interacts with a number of proteins, called together "Shelterin complex", which can influence chromosome end integrity and dynamics; it is crucial for t-loop formation and telomere protection. The shelterin complex is composed by six proteins, TRF1 and TRF2 (telomeric repeat binding factor 1 and 2), RAP1 (repressor activator protein 1), TIN2 (TRF1-interacting protein 2), TPP1 (Tripeptidyl peptidase 1) and POT1 (Protection of telomeres 1) (90, 108).

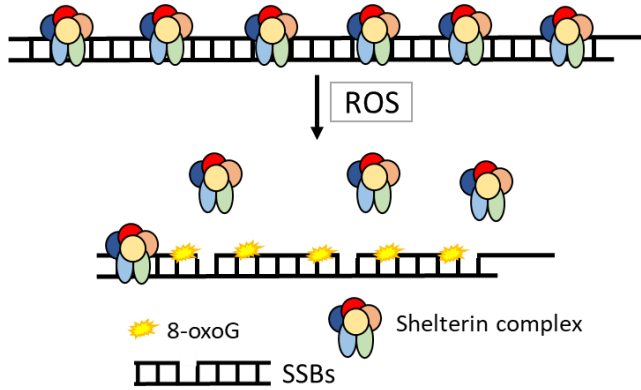

Figure 15 Oxidative stress induce the formation of oxidized bases in telomeric region. *This could lead to SSBs formation, telomere shortening and reduce the binding of telomeric proteins. Modified by (111).*

3.4 DNA Damage Response (DDR)

After DNA damage detection the DDR pathway directs the DNA-repair activities and arrests the cell-cycle progression in proliferating cells until the DNA damage has been completely repaired (112). The activation of the DDR can be detected through the association of DNA damage factors with the damaged chromatin, such as 53BP1[12] (p53 Binding Protein 1) (113), and to the phosphorylation of the histone variant H2AX (γH2AX) (114) (fig.16).

[12] 53BP1 is a protein involved in the detection and processing of DSBs (111).

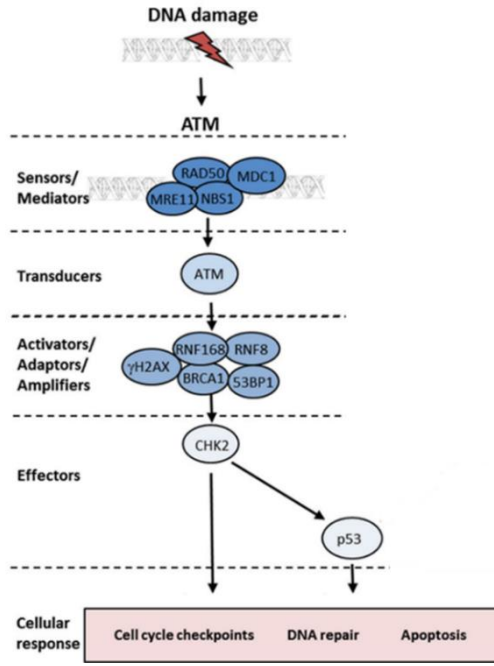

***Figure 16** The DNA damage signalling pathway of DNA DSBs.*
Changes in chromatin structure lead to the autophosphorylation of ATM, that localises to the DNA damage site and phosphorylates H2AX and 53BP1. Modified by (114).

In somatic cells, telomeres that reach the critical length could be recognized as DSBs and activate the DDR pathway, leading to senescence (65). The presence of the t-loop at the end of the chromosomes represses the activation of the DDR pathway, protecting chromosomes from end-to-end fusions (64, 76). Because of this, at telomere there are proteins involved in the DNA damage repair (64, 76) (fig.17).

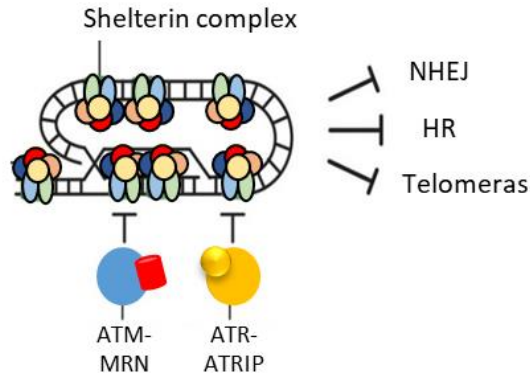

Figure 17 The shelterin complex, that form the t-loop, suppresses the activation of the DNA damage signaling and protects the end of chromosomes from end-to-end fusions and elongation. Modified by (76).

If telomeres are dysfunctional, the two DNA damage factors (53BP1 and γH2AX) are associated at telomeric regions, increasing the telomere-dysfunction induced foci (TIFs) (115).

4. AIM

Myotonic dystrophy (DM) is the most common muscular dystrophy in adults. It exists in two different forms, both caused by autosomal dominant nucleotide repeat expansions: a (CTG)n expansion in *Dystrophia Myotonica Protein Kinase* (*DMPK) gene* in DM1, a $(CCTG)_n$ expansion in *Zinc Finger Protein 9* (*ZNF9) gene* in DM2 (1-3). The expansions are transcribed in RNA, which forms secondary structures and sequesters RNA-binding proteins, forming nuclear aggregates that disturb DNA metabolism and require the involvement of DNA repair systems (1-3). In this thesis we will investigate about DM1, in which the DMPK gene has between 50 and several thousand of (CTG) repeats, while in healthy individuals contains between 5 and 38 repeats. Disease severity is directly proportional to the repeat size and indirectly proportional to the age of onset (1-3). In this disease, primarily high proliferative cells would have a higher tendency to expand DNA repeats, which contradicts the fact that the long tandem repeats are found in non proliferating (or less proliferating) post-mitotic tissues (2). In this regard, DNA repair mechanisms, especially Mismatch Repair (MMR) and Base Excision Repair (BER), also active in non-cycling cells, have been hypothesized to notably contribute to this phenomenon by amplifying the repeat expansion (2, 19, 29, 48).

Furthermore, literature proposes DM1 as a disease due to an increased susceptibility to oxidative stress (OS) with high levels of free radicals and reduced cellular antioxidant activity (42, 43) with a premature aging. Telomeres are biomarkers of senescence (61). DM1 affected satellite cells seem having a higher telomere shortening rate (2, 59), but this does not seem to be related to the pathology (2, 59). Considering that proteins involved in telomere homeostasis regulation could also participate to the DDR (59, 76), it could be that the large $(CTG)_n$ expanded repeats may recruit telomeric/repair proteins leading to unstable chromosome ends, accelerating telomeres shortening (59). . It is also known that telomere shortening is associated with higher OS levels (77). Furthermore, the cellular susceptibility to OS is positively correlated with the number of (CTG) repeats (58). However, it still remains to understand if $(CTG)_n$ repeat expansion could interfere with telomere homeostasis.

Because up to now data showed in literature are pretty clinical, there is still a lot to understand about the mechanisms and the target

involved in this disease. Concerning this, the aim of this project is to understand the pathway activated and any target involved in this disease, considering also the higher oxidative stress in DM1 patients.
To reach this purpose, in order to evaluate the response to DNA damage and the repair systems, after having characterized DM1 primary fibroblasts, we treated them and healthy control fibroblasts (WT) with different genotoxic agent: hydrogen peroxide (H_2O_2) (200 µM) and X-rays (2Gy). After different times post treatment, we have evaluated several endpoints:

- karyotype of DM1 patients after X-rays (2Gy);
- DNA damage and ANMs after H_2O_2 treatment (200µM, 1 hr);
- DDR activation;
- telomeric oxidative damage;
- cell growth rate, viability and senescence.

5. RESULTS

5.1 DM1 cells $(CTG)_n$ repeat expansion size characterization

DM1 is a disease caused by autosomal dominant $(CTG)_n$ repeat expansion in *Dmpk gene* (1-3). The *Dmpk* gene of healthy individuals contains between 5 and 38 repeats, while repeat length of 38-50 are considered premutation alleles; DM1 affected individuals have between 50 and several thousand of $(CTG)_n$ repeats (1-3). Disease severity increases while age of onset decreases with an increasing number of repeats (1-3). In this work, we used human primary fibroblasts derived from skin biopsies of DM1 patents (5 or 6 patients) and healthy people as control (WT) (2 or 3 healthy people) (University of Rome Tor Vergata). We characterized our cells following the best practice guideline for DM1 and DM2 molecular diagnosis (116). Firstly, conventional PCR and fragment-length analysis were performed in order to discriminate cells that have two alleles with a low number of repeats (predominantly healthy) from those in which only one allele size is detected (DM1 patients or healthy). Subsequent techniques were used to detect possible repeat expansions: Triplet-repeat Primed (TP)-PCR (fig.18A) and Southern blotting of Long-range-PCR (fig.18B) in order to determine the $(CTG)_n$ expansion size range. Table 2 shows our DM1 patients $(CTG)_n$ repeat expansion size.

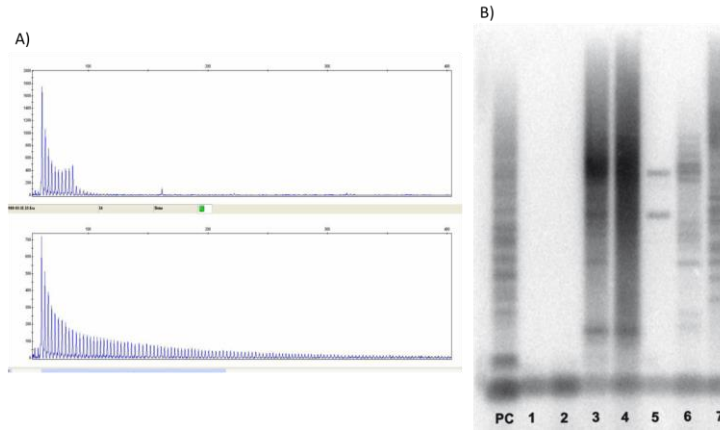

Figure 18 DM1 primary fibroblasts $(CTG)_n$ repeat expansion characterization. *A) Fragment-length analysis of TP-PCR products of the CTG repeat in the DMPK gene. Fluorescently-labelled PCR products of a representative healthy individual having two normal alleles (top panel) and a representative affected individual (bottom panel); B) Southern blotting of long-range PCR-products of the CTG repeat in the DMPK gene. Long-range PCR fragments were subjected to agarose gel electrophoresis and capillary transfer to a nylon membrane. Subsequently, the membrane was hybridized with a labeled $(CAG)_5$ probe. Visualized repeats were from 2 representative healthy control (lane 1-2), and 5 patients with a heterozygous expansion (lane 3-7), positive control (PC).*

Table 2 DM1 fibroblasts (CTG)n repeat expansion size.

DM1 patients	**$(CTG)_n$ repeat expansion size**
DM1_A	400-720
DM1_B	436-650
DM1_C	560-920
DM1_D	500-1200
DM1_E	118
DM1_F	600-800

5.2 Mismatch repair (MMR) and Base Excision Repair (BER) systems are less expressed in DM1 fibroblasts respect to healthy control cells

DNA tandem repeats acquire secondary structure (19, 24, 30) resulting as substrate for DNA damage response (DDR) (18, 19, 23-25, 28, 29). As previously introduced (section 3.1.1), MMR and BER DNA repair mechanisms have been shown to significantly contribute to trinucleotide-repeats expansion (19, 29, 41).

In order to evaluate the basal level of the genes involved in these two pathways, we performed Real-time qPCR using custom cards (ThermoFisher Scientific, Massachusetts, USA) that allowed us to evaluate all the genes involved in the MMR and BER pathways, at the same time. Our data, reported in figure 19, showed lower levels of all the MMR mRNAs we investigated in DM1 cells respect to WT, confirming the data obtained by Seriola et al. (33) on the down-regulation of the MMR components in differentiated DM1 human Embryonic Stem Cells (hESCs). In addition, we analyzed BER mechanism (fig.19), because involved in trinucleotide expansion (41), showing that also the genes of this repair system are lower translatedd in DM1 cells respect to WT.

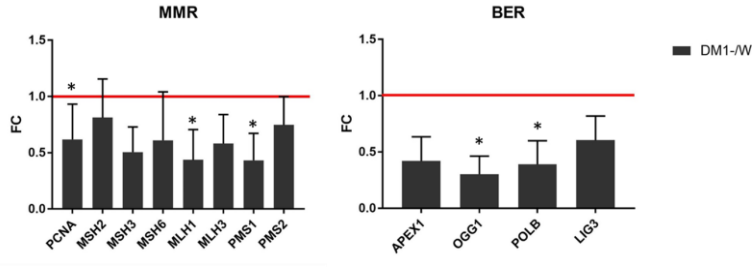

Figure 19 MMR and BER mechanisms pathways analysis.
*DM1 fibroblasts showed lower basal levels of all the genes involved in these two repair mechanisms: MMR (left panel) and BER (right panel). Data are shown in linear Fold Change (FC). The red line represents the WT-/WT- gene expression. Used 5 DM1 and 2 WT. Every data point was assessed from 1 experiment in 2 technical replicates and data are presented as means ± ES. Comparisons between multiple groups were made by t-student test. *p<0.05.*

5.3 X-ray induces a similar increase of aberration frequencies in both DM1 and WT

DNA damage could have serious consequences on cellular stability and viability if not properly repaired (80). The Double Strand Breaks (DSBs) probably represent the most dangerous lesions and are generated when the two complementary strands of the duplex DNA are broken, at the same time, at two different sites close to one another. In this case, the two DNA ends could not be juxtaposed; consequently, the two DNA ends dissociate from each other and the repair machinery cannot work correctly. This phenomenon gives the opportunity for inappropriate recombination with other sites in the genome leading to chromosome fusions (81). This kind of lesions are repaired by Homologous Recombination (HR) and Non-Homologous End Joining (NHEJ) repair systems, depending on the cell cycle phase (81). Ionizing radiation (IR) or radiomimetic drugs represent the most common inductor of DSBs (81).

To induce DSBs in order to study the behavior of the related repair systems, we irradiated our cells with X-rays (2Gy) and analyzed their karyotype after 24 hrs from the exposure. We performed Multicolor (M)-FISH, which allowed us to evaluate chromosome rearrangements (fig.20).

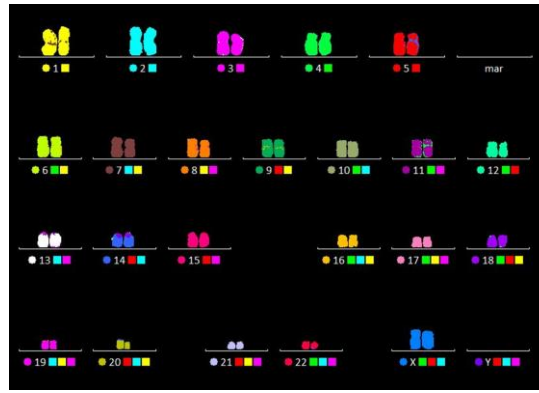

Figure 20 Example of m-FISH
Each chromosome has its unique fluorochrome profile.

Our data showed a similar behavior in response to X-ray irradiation in both DM1 and WT fibroblasts (fig.21) indicating that the increase of chromosome aberration due to IR exposure is similar in both samples.

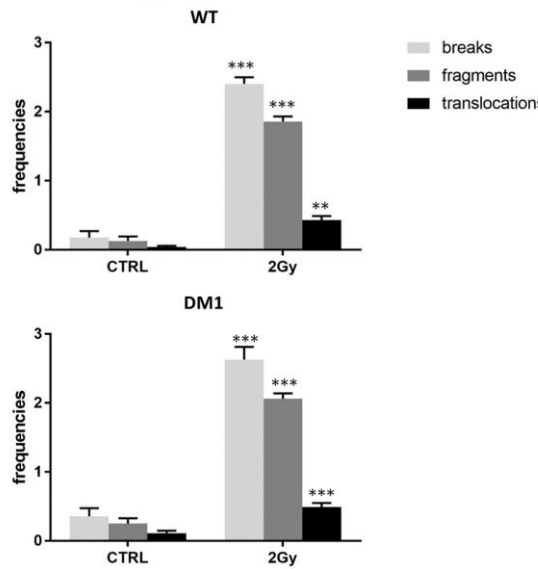

Figure 21 Chromosome aberrations induced by X-rays in DM1 and WT.
*Data obtained at 24 hrs after X-ray exposure (2Gy). DM1 fibroblasts showed a higher basal level of chromosome aberration respect to WT fibroblasts, but the aberration increase due to X-rays is similar in both samples. Used 5 DM1 and 3 WT. Every data point was assessed in 2 independent experiments and data are presented as means ± ES. Comparisons between multiple groups were made by t-student test. ***p<0.001; **p<0.01.*

5.4 Oxidative stress induces oxidative base damage that does not persist 24h after treatment both in WT and DM1 cells

The standard alkaline comet assay is a method used to investigate cellular DNA damage, in particular SSBs (fig.22).

The most frequent DNA damage induced by oxidative stress (OS) is base modification, and the principal product is 8-oxoG (108). For this reason, we performed the standard comet assay together with its formamidopyrimidine-DNA-glycosylase[13] (FPG)-modified version, which is more sensitive to the presence of oxidized bases.

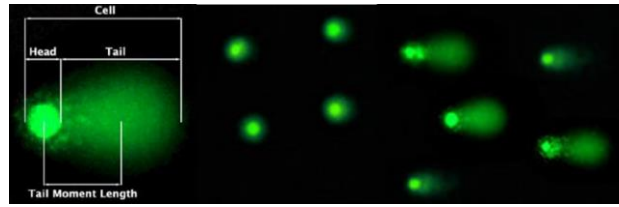

Figure 22 Example of comet assay.
The tail length is directly proportional to DNA damage amount

In figure 23 we show results obtained from comet assay. The standard comet assay (black portion of the columns) revealed in both DM1 and healthy cells an increase in DNA damage with 200 µM H_2O_2 compared to the untreated control immediately after treatment (0 hr) that decrease in time dependent manner. Both our untreated samples showed no DNA damage after FPG treatment (grey portion of the columns), only Standard comet assay reveal endogenous breaks (fig.23). The DNA damage observed in the FPG-modified comet assay (grey portion of the columns) in DM1 cells was statistically higher ($p<0.05$) than the one from the standard comet assay. Our data revealed a significant increase in FPG-modified comet assay also respect to untreated samples immediately after treatment (0 hr; $p<0.05$ in WT and $p<0.001$ in DM1 fibroblasts) and 5 hrs after treatment in both fibroblasts ($p<0.05$). 5 hrs after treatment our results indicate a genomic damage decrease.

[13] FPG is a glycolase able to recognize and specifically cut the oxidized bases, principally 8-oxoG from DNA, producing apurinic sites that will be converted in breaks by the associated AP-endonuclease activity (127).

A complete rescue of genomic damage was observed 24 hrs after treatment both with standard and FPG-modified comet assay, as evidenced by the similar values of treated samples and controls.

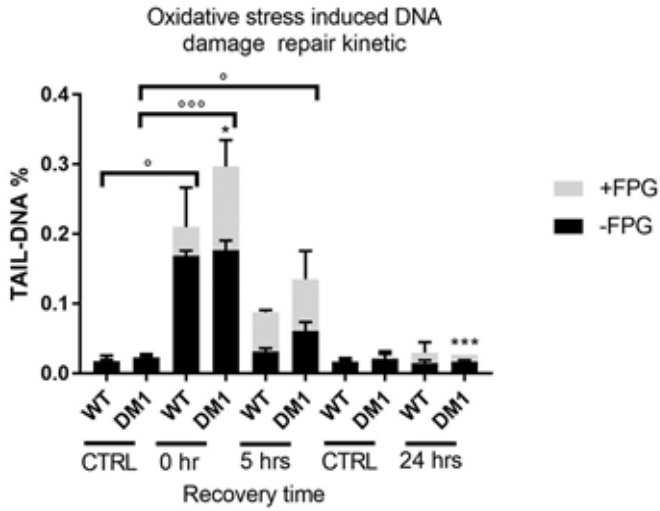

Figure 23 Standard and FPG-modified alkaline comet assay.
*Standard and FPG-modified versions of the comet assay have been used to evaluate the fold increase in genomic damage induced by H_2O_2 with respect to the control value. The net cleavage sites generated by FPG activity were calculated subtracting the value of total DNA damage yielded by the samples not treated with the enzyme from the DNA damage value obtained from samples treated with the enzyme. The value of this subtraction is shown in the graph as a light grey portion labelled "+FPG" To assess any changes in Tail DNA values, we analyzed control cells, immediately (0 hr) and after 5 hrs treatment. A significant increase ($p<0.05$) in FPG-modified comet assay is observed in the percentage of DNA damage immediately (0 hr) after treatment in DM1 fibroblasts compared to normal comet assay. We observed a time-dependent decrease of genomic damage to the control value 24 hrs after treatment. Used 6 DM1 and 3 WT. Every data point was assessed in 2 independent experiments and data are presented as means ± ES. Comparisons between multiple groups were made by t-student test. * indicates comparison between FPG-modified and standard comet assay at the same experimental time point. *$p<0.05$; ***$p<0.001$. ° indicates comparison between treated and untreated samples after FPG-modified comet assay °$p<0.05$; °°°$p<0.001$.*

5.5 DDR response analysis

Considering the higher damage observed in DM1 cells, to better characterize the response of our samples to 200 µM H_2O_2 (1 hr) we evaluated also the gene expression profile of some genes involved in BER and MMR by real- time qPCR. In particular, we have chosen the genes we found significantly down-regulated in DM1 respect to WT fibroblasts (paragraph 5.2, fig.19).

We tested 2 different experimental time points: 45 mins of treatment and 3 hrs after 1 hr of treatment, in order to evaluate both early and late times of mRNAs gene expression.

In particular, although there are no statistically significant differences between treated and untreated samples, generally we found a slight induction of mRNA levels at 45 mins of treatment in both samples and a decrease of their transcripts 3 hrs after treatment (fig.24).

These results obtained by gene expression analysis are in agreement with the oxidative stress DNA damage repair kinetic evaluated by comet assay (fig.23) in which we found a decrease of both genomic and oxidative DNA damage between the end of the treatment and 5 hrs of recovery.

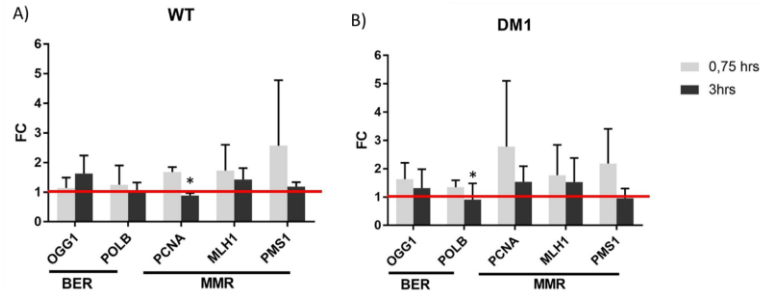

Figure 24 Gene expression profile induced by 200 µM H_2O_2 treatment in DM1 and WT fibroblasts at different time points.

*Data showed an increase of mRNAs levels of all gene tested induced by treatment both in DM1 and WT fibroblasts. Gene expression profile in WT fibroblasts (A) and DM1(B). Data are showed in linear Fold Change (FC). Used 5 DM1 and 2 WT. Every data point was assessed in 2 technical repeats and data are presented as means ± SD. Comparisons between treated and untreated samples were made by t-student test. *p<0.05.*

5.6 Abnormal nuclear morphology (ANMs) induction as a measure of chromosome instability induced by oxidative stress

To assess chromosome instability (CIN) we analyzed MN, NPBs and NBUDs (86) (fig.25) in binucleated cells (BN), biomarkers of chromosome instability as a result of H_2O_2 treatment (200 μM; 48 and 72 hrs) (fig.25).

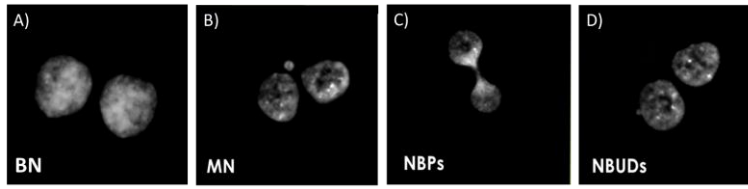

Figure 25 Examples of chromosome instability biomarkers.
Representative images of (A) Binucleated (BN) cells with different abnormal nuclear morphologies. (B) Micronucleus (MN), (C) Nucleoplasmic Bridge (NPBs), (D) Nuclear Buds (NBUDs).

The results revealed a greater increase of ANMs 48 hrs after treatment (fig.26) for both cells. Interestingly DM1 cells showed a little more baseline ANMs than WT cells, probably due to a higher intrinsic chromosome instability in these patients, both at 48 and 72 hours. On the contrary, the induction of damage due to H_2O_2 treatment resulted to be higher in DM1 at 48 hrs but similar in both samples at 72 hrs (fig.26).

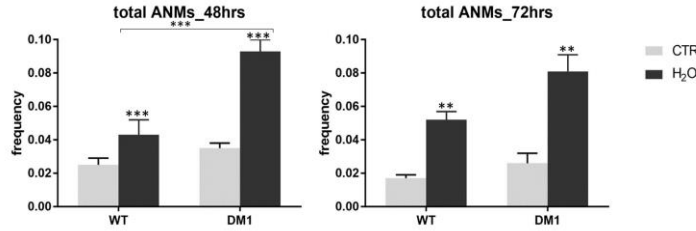

Figure 26 ANMs frequencies induced by H_2O_2 treatment at 48 and 72 hrs.
*Total Abnormal Nuclear Morphologies (ANMs) at 48 hrs (on the left side), and at 72 hrs (on the right side) after 200 μM H_2O_2 treatment. Our data showed a higher baseline of ANMs frequency in DM1 cells at both the experimental time points, while we obtained a greater increase in DM1 cells respect to WT ones at 48 hrs followed by a similar behavior at 72 hrs. Every data point was assessed in 2 independent experiments and data are presented as means ± ES. Comparisons between multiple groups were made by t-student test. **p<0.01; ***p<0.001.*

More specifically (fig.27), WT cells showed lower frequencies (top panel) of MN, NPBs and NBUDs induced by H_2O_2 treatment, at 48 hrs and 72 hrs, than those observed in DM1 cells (bottom panel). MN seemed to have a time-dependent increase in concomitant with a decrease of the NBUDS and NPBs.

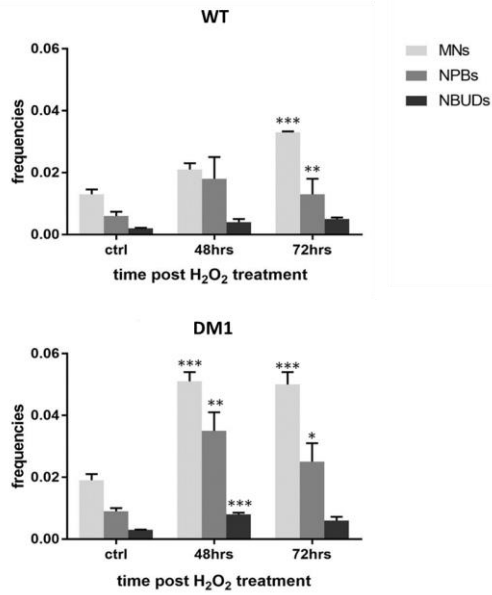

Figure 27 ANMs frequencies induced by H_2O_2 treatment at 48 and 72 hrs.
*The different columns denote the abnormal nuclear morphologies analyzed (NPBs, MN and NBUDs) at different times, compared to the control data. They both showed an increase of ANMs, although WT fibroblasts seemed to have a slower kinetic. (on top) in WT fibroblasts we observed a low increase of ANMs frequencies. (on bottom) in DM1 fibroblasts we observed a higher and faster increase of all the biomarkers. Used 5 DM1 cell lines and 3 WT cells lines. Every data point was assessed in 2 independent experiments and data are presented as means ± ES. Comparisons between multiple groups were made by t-student test. *p<0.05; **p<0.01; ***p<0.001.*

5.7 Hydrogen peroxide induces a slight decrease of telomere length but a higher increase of γH2AX telomere dysfunction-induced foci (TIFs) in DM1 fibroblasts

We performed telomere length analysis by Quantitative (q)-FISH (fig.28) to test whether 200 μM H_2O_2 treatment induced telomere shortening, because oxidative stress is known to induce telomere shortening (77, 107).

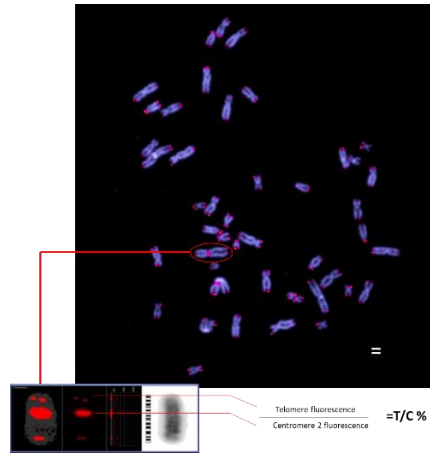

Figure 28 Example of q-FISH.
Quantitative-Fluorescence in situ Hybridization analysis. Telomere lengths (T/C%) were calculated as the ratio between the total telomeres fluorescence (T) and the fluorescence of the centromere of the two chromosomes 2 (C), used as the internal reference in each metaphase analyzed.

The analysis of telomere length is showed in figure 28. As previously showed by Bigot et al. (2, 59), untreated DM1 fibroblasts showed 25% shorter telomeres respect to WT (fig.29A,B). 48 hrs after H_2O_2 treatment we observed 22% ($p<0.01$) telomere shortening in WT fibroblasts (fig.29C,D) ($p<0.01$), and 17% in DM1 (fig.29E,F) ($p<0.05$).

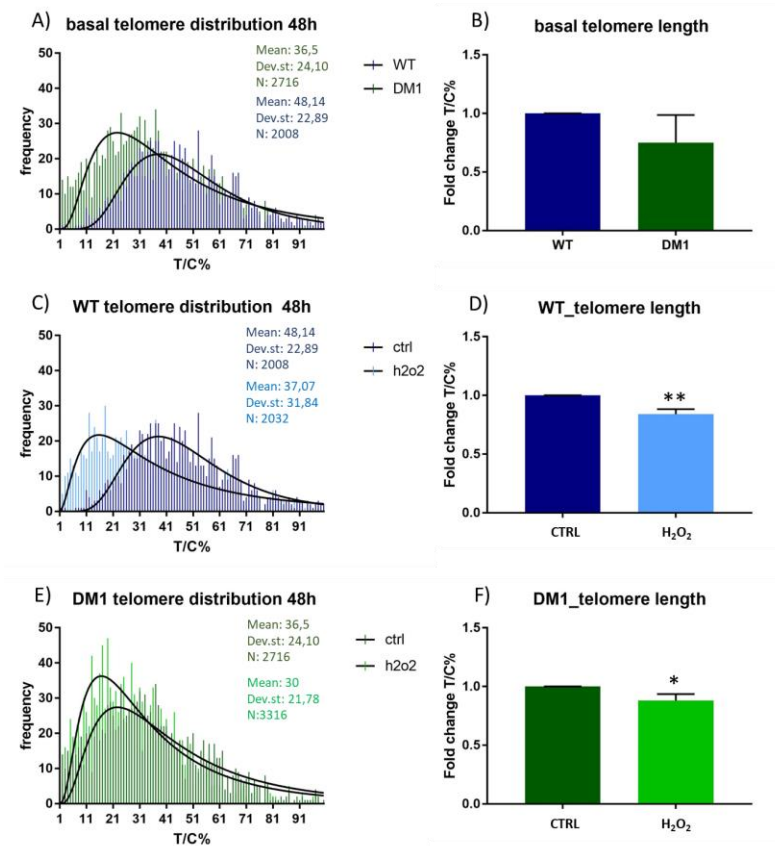

Figure 29 Telomere length in DM1 and WT.

*On the left side representative distributions of telomere length. On the right side, histograms representing results obtained by telomere length analysis. A) Representative Comparison between basal telomere distribution in DM1 and WT fibroblasts; B) DM1 telomeres are 25% shorter than WT telomeres. C) Representative Comparison between telomere distribution of treated and untreated WT fibroblast; D) histogram shows a reduction of 22% in WT telomere length 48 hrs after treatment. E) Representative Comparison between telomere distribution of treated and untreated DM1 fibroblasts; F) histogram shows a reduction of 17% in DM1 telomere length 48 hrs after treatment. Used 5 DM1 and 3 WT. Every data point was assessed in 3 independent experiments and data are presented as means ± ES. Comparisons between multiple groups were made by t-student test.*p<0.05; **p<0.01).*

In somatic cells, telomeres that reach the critical length could be recognized as DSBs and activate the DDR pathway, leading to senescence (65). To evaluate the activation of the DDR at telomeric level after OS, we performed a co-immunofluorescence staining with a marker of damage at telomeres, the phosphorylated form of H2AX (γH2AX) and the shelterin complex protein TRF1, which specifically bind telomeric region (fig.30). The co-localization between these two proteins detects the telomere dysfunction-induced foci (TIFs) (fig.30).

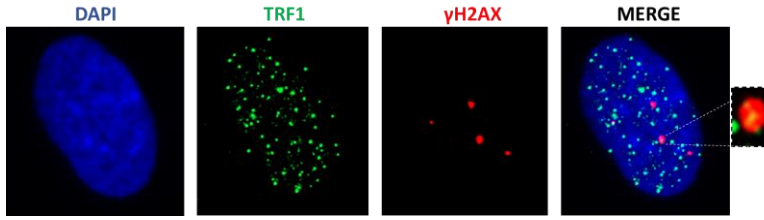

Figure 30 Example of co-immunofluorescence of TRF1 and γH2AX proteins.
Images of fibroblast stained for telomeric shelterin protein TRF1 (green spots) and γH2AX foci (red spots). Co-localization of both signals (green and red spots) indicates the presence of a telomere dysfunction-induced focus (TIF). More than a single telomeric TRF1 signal can co-localize with a single γH2AX focus. TIF (last boxes) are enlarged to show the co-localization between γH2AX and TRF1.

Results obtained are shown in figure 31. It is interesting to note that DM1 cells showed a slight high basal level of co-localization respect to WT (even if they are not statistically significant), and this could be correlated to the shorter basal telomere length. We also observed a significant increase ($p<0.05$) of γH2AX TIFs 48 hrs after treatment for DM1 fibroblasts, while a lower increase was observed in WT ones (fig.31).

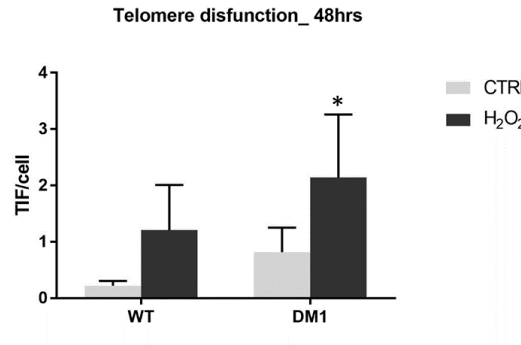

Figure 31 Telomere dysfunction-induced γH2AX foci (TIFs).
The graph represents results of telomeric damage after oxidative stress in WT and DM1 fibroblasts. The columns evidence data obtained by co-localization between γH2AX foci and telomere TRF1 per cell. We observed a significant increase ($p<0.05$) of foci 48 hrs after treatment for DM1 fibroblast, while WT showed a slight increase.
*Statistical analysis was performed between treated and control samples. Used 5 DM1 and 2 WT. Every data point was assessed in 2 independent experiments and data are presented as means ± ES. Comparisons between multiple groups were made by t-student test. *$p<0.05$.*

5.8 Oxidative stress induces a decrease in cell growth rate correlated to an increase of senescence both in DM1 and WT cells

To evaluate if H_2O_2 treatment could induce a cellular selection, we performed a cell growth curve (fig.32A-B). For both DM1 and WT cells, we observed a significant growth delay starting 48 hrs after treatment ($p<0.05$) and persisting up to 168 hrs (fig.32A-B). Cell viability was not different between both DM1 and WT treated and untreated cells (fig.32C). Our data did not show a significant viability decrease after treatment, suggesting a cell proliferation arrest induced by H_2O_2 in both our samples.

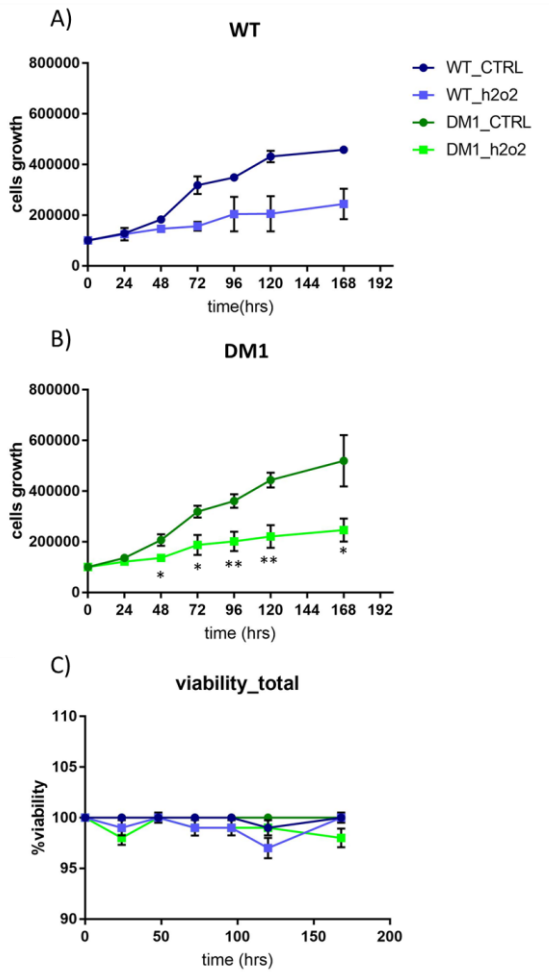

Figure 32 Cellular growth rate and viability.
DM1 and WT primary fibroblasts were treated with 200 µM H_2O_2. After treatment (1hr), cells were seeded (t_0) at a density of 10^5 and harvested every 24 hrs up to 168 hrs. Total cells were counted using Burker's chamber (A-B), and the percentage of viable cells was determined by trypan blue assay (C). Used 5 DM1 patient cells and 2 WT cells. Every data point was assessed in 2 independent experiments and data are presented as means ± ES. Comparisons between multiple groups were made by t-student test. *p < 0.05; **p<0.01.

Because of the similar cell proliferation arrest and the increase of TIFs in both normal and DM fibroblasts, we decided to test if H_2O_2 treatment could induce premature cell senescence. Therefore, we used a β-galactosidase staining kit to evaluate the senescent cells percentage (fig.33). β-galactosidase is in fact a hydrolyzing enzyme that catalyzes the hydrolysis of β-galactoside into monosaccharides only in senescent cells (117); using the staining assay at pH 6 only senescent cells develop blue color (fig.33).

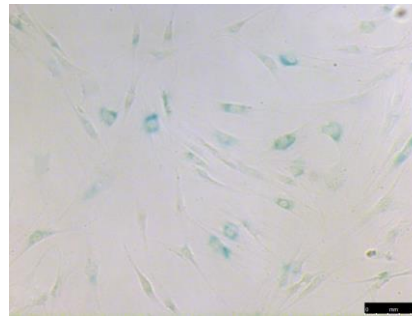

Figure 33 Example of senescence β-galactosidase staining.
The blue cells are positive to the senescence marker.

We evaluated the frequency of senescent cells at 48 and 96 hrs after 200 μM H_2O_2 treatment and figure 35 shows the results we obtained. Both WT and DM1 cells showed 20% senescent cells in control samples (fig.34). After 48 hrs from treatment the increase of senescent cells is slightly high in DM1 cells ($p<0.001$) than in WT; at 96 hrs we have a significant increase of senescent cells in DM1 cells (65%, $p<0.001$) (fig.34).

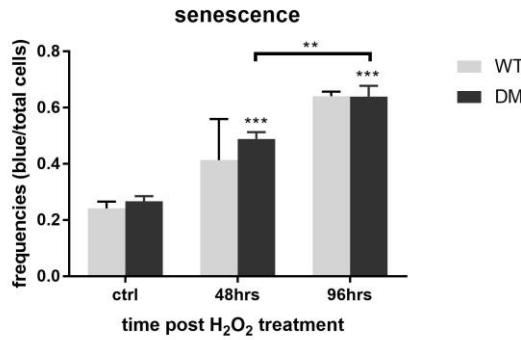

Figure 34 Senescence β-galactosidase staining in WT and DM1 fibroblasts at 48 and 96 hrs.

*The graph represents results of premature induced senescence in WT and DM1 fibroblasts after 48 and 96 hrs after 200 µM H_2O_2 treatment. The columns evidence frequency of senescent cells (blue cells/tot cells counted). Both normal and DM1 cells showed the same increase of senescence induced by treatment and the increase is time dependent. Statistical analysis was performed between treated and control samples. Used 5 DM1 and 2 WT. Every data point was assessed in 2 independent experiments and data are presented as means ± ES. Comparisons between multiple groups were made by t-student test. ***p<0.001; **p<0,01.*

6. DICUSSION

Myotonic Dystrophy type 1 (DM1) is a multisystemic disease caused by an unstable trinucleotide (CTG) repeat motif expansion in the 3' untranslated region (UTR) of the *Dystrophia Myotonica Protein Kinase (Dmpk)* gene, located on chromosome 19q13.3 (1-3) and has a frequency of 1 of 8000 individuals worldwide (2, 3, 6, 7). The length of $(CTG)_n$ repeats is inversely correlated with the age of onset of the disease and consequently with its severity (1-3, 8, 12, 13). DM1 disease is characterized by *somatic mosaicism*: the existence of cells with different expansion length within an organism (1-3). In fact, some tissues and cell types possess a higher tendency to extend these tandem repeats sequences. The longest tandem repeats have been found in severely affected tissues (2, 8, 12-15). Furthermore, DM1 has been proposed as a disease due to premature aging and free radical production (2, 42, 43) and there are evidences that the susceptibility to oxidative stress (OS) is $(CTG)_n$ repeats number-dependent (57, 58).
MMR protein complex in particular MSH2, MSH3 and PMS2, and BER components such us OGG1 can interact and cooperate to increase trinucleotide repeats instability (29, 33, 41, 47, 49). In particular MMR pathway is involved in repairing secondary structure acquired by DNA, while BER pathway is involved in repairing modified basis such as 8-oxo-G prevalently induced by OS.
A direct prove of the implication of MMR components in trinucleotide expansion in DM1 has been demonstrated by Seriola et al. (33) who for the first time has shown the down-regulation of the MMR components in differentiated DM1 human hESCs in concomitant with the stabilization of the $(CTG)_n$ expansion size (33). On the other hand, there are no direct evidences about an involvement of BER pathway in this disease.
Starting from these few knowledges, we wanted to understand the mechanisms, pathways and target involved in this disease.
In order to reach this purpose we first characterized our fibroblasts. After having quantified their $(CTG)_n$ expansion size, we have evaluated the gene expression profile of MMR and BER mechanism components. As expected for MMR system we found a down-regulation of its all components in DM1 cells respect to WT confirming Seriola et al. (33). In this thesis, we also obtained data on basal expression levels of BER components in differentiated DM1

cells. In particular, DM1 fibroblasts showed a lower gene expression profile of all the BER components investigated. These results allowed us to demonstrate in fibroblasts the low basal levels of gene expression of these two DNA repair mechanisms, involved in trinucleotide-repeat expansion typical of this disease, and this could be related to the higher intrinsic instability demonstrated for all our endpoints (tab.3).

Table 3 Intrinsic genomic instability in WT and DM1 cells per each endpoint.

	Chromosome aberration at 24 hrs (aberration/metaphase)	ANMs mean frequency at 48 and 72 hrs (ANMs/BN)	Telomere length at 48 hrs (T/C%)	γH2AX TIFs at 48 hrs (TIFs/cell)
WT	0.34	0.21	54.7	0.22
DM1	0.72	0.31	40.8	0.81

Therefore, in order to evaluate the response of these cells to induced DNA damage, we decided to treat our samples with two different genotoxic agents. In particular, we treated fibroblasts with 2 Gy of IR. IR represents one of the most common inductor of DSBs (81). The DSBs probably represent the most dangerous lesions and are repaired by HR and NHEJ, depending on the cell cycle phase (81).
In order to evaluate these two repair mechanisms, we analyzed DM1 and WT karyotypes after 24 hrs from the exposure. Our data showed a similar behavior after X-ray irradiation in both DM1 and WT fibroblasts, although triplet expansion induces higher level of genomic instability. These results support the idea that DNA DSBs repair is not involved in repeat expansion, in mammalian systems (41).
On the contrary, the H_2O_2 treatment allowed us to evaluate MMR and BER working. The principal DNA damage induced by oxidative stress is the modification of DNA bases such as 8-oxoG that could be repaired correctly both by BER and MMR systems (100-103, 118, 119), or if not, it could induce single or double strand breaks and GC-AT mutation (101). To assess the whole genome DNA damage induced by the acute OS treatment comet assay revealed an induction of DNA damage that rescue in a time dependent manner indicating that genomic damage was repaired in 24 hrs both in DM1 and WT fibroblasts (although in DM1 fibroblasts we found a higher DNA damage induction). The analysis of gene expression profile of MMR and BER genes allowed us to evidence that these genes are significantly down-regulated at basal level in DM1 fibroblasts, but

their activation after DNA damage induction was similar to the WT samples, revealing us that MMR and BER mechanisms works correctly in DM1 fibroblasts.
The analysis of other CIN biomarkers, in particular the Abnormal Nuclear Morphologies (ANMs) represented by Micronuclei (MN), Nuclear Buds (NBUDs) and Nucleoplasmic Bridges (NPBs) (87) after H_2O_2 revealed a greater increase of ANMs 48 hrs after treatment (especially in DM cells) persisting up to 72 hrs. Interestingly DM1 fibroblasts showed a higher baseline number of ANMs than WT, due probably to a higher intrinsic chromosome instability in these patients.
These results were in contradiction with our previous results in which we demonstrated that all the genomic oxidative DNA damage induced by H_2O_2 treatment was repaired within 24 hrs. Recently, some authors have demonstrated that ANMs could be associated also with telomere dysfunction (77, 91). In fact, Pampalona et al., (91) have proposed that in particular the NPBs derive from end-to-end fusions, affecting chromosomes with critically short telomeres that lead to chromosome-end-fusions, visible as NPBs in interphase.
For this reason, we investigated telomere length in DM1 and WT fibroblasts. As expected, DM1 showed shorter telomeres respect to WT, confirming literature data (59, 68). After treatment, WT and DM1 fibroblasts showed a telomere length reduction as expected (77), even if the telomere shortening seems more evident in WT than in DM1 fibroblasts. These results could be due to the basal shorter telomeres present in DM1 and induced OS probably could not be able to further shorten the chromosome ends; in our idea, a shortening threshold of telomere exists and cells that exceed this threshold could die. Furthermore, because the role of telomere could be influenced not only by telomere length but also by telomere structure maintenance (65, 79, 110), in order to understand if DM1 telomeres are dysfunctional we evaluated the frequency of TIFs. This analysis showed a significant increase of γH2AX TIFs 48 hrs after treatment for DM1 fibroblasts and a lower increase in WT ones. Also in this analysis, DM1 fibroblasts showed a higher baseline level of TIFs probably due to the shorter telomeres. These results well correlates with the increased number of NPBs we found at 48 hrs from treatment and with the consequent increase of MN and NBUDs at 72 hrs due to

the NPBs breaks. The short telomere length we found in DM1 untreated fibroblasts also justify the higher basal levels of NPBs in these cells.
All these data strongly correlate with the finding reported in Coluzzi et al, 2014, in which in MRC-5 fibroblasts treated with H_2O_2 an increase of γH2AX TIFs is correlated with a telomere shortening and with an increase of NPBs at 48 hrs that give rise to MN and NBUDs at 72 hrs (77). Also in this case the genomic FPG-comet assay showed a total rescue of the oxidative DNA damage within 24 hrs, but the FPG-sensitive base lesions within telomeric DNA revealed a significant persistence of oxidative DNA damage, probably 8-oxoG, at telomeric regions after 24 hrs from treatment suggesting that oxidative DNA damage repair may be less effective in telomeres (77).
This allow us to hypothesize that also in our cells this phenomenon could occur and that at telomere level probably the oxidative damage could persist inducing the telomere dysfunction observed and the related ANM observed (in DM1 cells more than in WT).
Because of the role of telomeres in cellular growth and senescence (65), these two end-points were studied. We observed a strong proliferative arrest in DM1 that persist until 168 hrs. These results were strongly support by the senescence β-galactosidase staining that revealed in DM1 a statistically significant senescent cells confirming the role of telomeres in this disease.
The aim of this thesis was to try to understand the biological mechanisms involved in the development of the disease and the probable marker(s) involved. Unfortunately, we realize the limit of this research due to the few samples, but it is important to stress that in rare disease field is really difficult to collect a big number of samples from affected people and, most of all, it is really difficult to collect normal controls because of the invasiveness of the sample collection (e.g. tissue biopsy). Considering this, in spite of simple size, analyze many different endpoints could help to have an overview of the disease, which allow to try to better comprehend the etiopathological mechanisms of these rare diseases, although the low significant differences.

7. CONCLUSION

In rare disease field is really difficult to collect a big number of samples from affected people and, most of all from normal controls because of the invasiveness of the sample collection. Considering this, the analysis of many different endpoints could help to have an overview of the disease. In fact the comprehension of the mechanisms of these rare disease takes on an important contribution to these disease knowledge and get the bases for future researches. In this work we have evaluated the response of fibroblasts derived from DM1 patients to different genotoxic agents. We found that DM1 cells show a higher intrinsic level of genomic instability but also a higher increase of DNA damage induced by H_2O_2 mostly at telomeric region, as supported by the higher levels of ANMs and TIFs respect to WT. Surprisingly, these cells proliferate and undergo in senescence like the WT cells. This allow us to hypothesize that probably DM1 fibroblasts could have a less regulated cell cycle checkpoint that allow a DNA damage that normal cells would not tolerate. On the other hand, considering the high rate of senescent cells, it could be interesting to analyze the destiny of these cells both in DM1 and WT at longer time, in order to evaluate if they are able to recover the proliferative block or if they die. There is still a lot of work to do to better understand the mechanisms involved in this disease but the evaluation of cell cycle and its regulation could be one of the first analyses to perform.

8. BIBLIOGRAPHY

1. Cho DH, Tapscott SJ. Myotonic dystrophy: emerging mechanisms for DM1 and DM2. Biochimica et biophysica acta. 2007;1772(2):195-204.
2. Mateos-Aierdi AJ, Goicoechea M, Aiastui A, Fernandez-Torron R, Garcia-Puga M, Matheu A, et al. Muscle wasting in myotonic dystrophies: a model of premature aging. Frontiers in aging neuroscience. 2015;7:125.
3. Udd B, Krahe R. The myotonic dystrophies: molecular, clinical, and therapeutic challenges. The Lancet Neurology. 2012;11(10):891-905.
4. Liquori CL, Ricker K, Moseley ML, Jacobsen JF, Kress W, Naylor SL, et al. Myotonic dystrophy type 2 caused by a CCTG expansion in intron 1 of ZNF9. Science. 2001;293(5531):864-7.
5. Ricker K, Koch MC, Lehmann-Horn F, Pongratz D, Otto M, Heine R, et al. Proximal myotonic myopathy: a new dominant disorder with myotonia, muscle weakness, and cataracts. Neurology. 1994;44(8):1448-52.
6. Lopez de Munain A, Blanco A, Emparanza JI, Poza JJ, Marti Masso JF, Cobo A, et al. Prevalence of myotonic dystrophy in Guipuzcoa (Basque Country, Spain). Neurology. 1993;43(8):1573-6.
7. Mathieu J, Prevost C. Epidemiological surveillance of myotonic dystrophy type 1: a 25-year population-based study. Neuromuscular disorders : NMD. 2012;22(11):974-9.
8. Udd B, Meola G, Krahe R, Thornton C, Ranum LP, Bassez G, et al. 140th ENMC International Workshop: Myotonic Dystrophy DM2/PROMM and other myotonic dystrophies with guidelines on management. Neuromuscular disorders : NMD. 2006;16(6):403-13.
9. Du H, Cline MS, Osborne RJ, Tuttle DL, Clark TA, Donohue JP, et al. Aberrant alternative splicing and extracellular matrix gene expression in mouse models of myotonic dystrophy. Nature structural & molecular biology. 2010;17(2):187-93.
10. Wheeler TM, Thornton CA. Myotonic dystrophy: RNA-mediated muscle disease. Current opinion in neurology. 2007;20(5):572-6.
11. Harper PS. Congenital myotonic dystrophy in Britain. I. Clinical aspects. Archives of disease in childhood. 1975;50(7):505-13.
12. Ashizawa T, Sarkar PS. Myotonic dystrophy types 1 and 2. Handbook of clinical neurology. 2011;101:193-237.

13. Martorell L, Monckton DG, Gamez J, Johnson KJ, Gich I, Lopez de Munain A, et al. Progression of somatic CTG repeat length heterogeneity in the blood cells of myotonic dystrophy patients. Human molecular genetics. 1998;7(2):307-12.
14. Anvret M, Ahlberg G, Grandell U, Hedberg B, Johnson K, Edstrom L. Larger expansions of the CTG repeat in muscle compared to lymphocytes from patients with myotonic dystrophy. Human molecular genetics. 1993;2(9):1397-400.
15. Thornton CA, Johnson K, Moxley RT, 3rd. Myotonic dystrophy patients have larger CTG expansions in skeletal muscle than in leukocytes. Annals of neurology. 1994;35(1):104-7.
16. Monckton DG, Wong LJ, Ashizawa T, Caskey CT. Somatic mosaicism, germline expansions, germline reversions and intergenerational reductions in myotonic dystrophy males: small pool PCR analyses. Human molecular genetics. 1995;4(1):1-8.
17. Timchenko L, Monckton DG, Caskey CT. Myotonic dystrophy: an unstable CTG repeat in a protein kinase gene. Seminars in cell biology. 1995;6(1):13-9.
18. Pearson CE, Nichol Edamura K, Cleary JD. Repeat instability: mechanisms of dynamic mutations. Nature reviews Genetics. 2005;6(10):729-42.
19. Jones L, Houlden H, Tabrizi SJ. DNA repair in the trinucleotide repeat disorders. The Lancet Neurology. 2017;16(1):88-96.
20. Schmidt MH, Pearson CE. Disease-associated repeat instability and mismatch repair. DNA repair. 2016;38:117-26.
21. Yum K, Wang ET, Kalsotra A. Myotonic dystrophy: disease repeat range, penetrance, age of onset, and relationship between repeat size and phenotypes. Current opinion in genetics & development. 2017;44:30-7.
22. Du J, Campau E, Soragni E, Jespersen C, Gottesfeld JM. Length-dependent CTG.CAG triplet-repeat expansion in myotonic dystrophy patient-derived induced pluripotent stem cells. Human molecular genetics. 2013;22(25):5276-87.
23. McMurray CT. DNA secondary structure: a common and causative factor for expansion in human disease. Proceedings of the National Academy of Sciences of the United States of America. 1999;96(5):1823-5.

24. McMurray CT. Mechanisms of trinucleotide repeat instability during human development. Nature reviews Genetics. 2010;11(11):786-99.
25. Wells RD. Molecular basis of genetic instability of triplet repeats. The Journal of biological chemistry. 1996;271(6):2875-8.
26. Kovtun IV, Goellner G, McMurray CT. Structural features of trinucleotide repeats associated with DNA expansion. Biochemistry and cell biology = Biochimie et biologie cellulaire. 2001;79(3):325-36.
27. Kovtun IV, McMurray CT. Trinucleotide expansion in haploid germ cells by gap repair. Nature genetics. 2001;27(4):407-11.
28. Pearson CE, Ewel A, Acharya S, Fishel RA, Sinden RR. Human MSH2 binds to trinucleotide repeat DNA structures associated with neurodegenerative diseases. Human molecular genetics. 1997;6(7):1117-23.
29. Iyer RR, Pluciennik A, Napierala M, Wells RD. DNA triplet repeat expansion and mismatch repair. Annual review of biochemistry. 2015;84:199-226.
30. Mirkin SM. Expandable DNA repeats and human disease. Nature. 2007;447(7147):932-40.
31. Lopez Castel A, Cleary JD, Pearson CE. Repeat instability as the basis for human diseases and as a potential target for therapy. Nature reviews Molecular cell biology. 2010;11(3):165-70.
32. Panigrahi GB, Slean MM, Simard JP, Gileadi O, Pearson CE. Isolated short CTG/CAG DNA slip-outs are repaired efficiently by hMutSbeta, but clustered slip-outs are poorly repaired. Proceedings of the National Academy of Sciences of the United States of America. 2010;107(28):12593-8.
33. Seriola A, Spits C, Simard JP, Hilven P, Haentjens P, Pearson CE, et al. Huntington's and myotonic dystrophy hESCs: down-regulated trinucleotide repeat instability and mismatch repair machinery expression upon differentiation. Human molecular genetics. 2011;20(1):176-85.
34. Slean MM, Panigrahi GB, Ranum LP, Pearson CE. Mutagenic roles of DNA "repair" proteins in antibody diversity and disease-associated trinucleotide repeat instability. DNA repair. 2008;7(7):1135-54.
35. Manley K, Shirley TL, Flaherty L, Messer A. Msh2 deficiency prevents in vivo somatic instability of the CAG repeat in

Huntington disease transgenic mice. Nature genetics. 1999;23(4):471-3.
36. Savouret C, Brisson E, Essers J, Kanaar R, Pastink A, te Riele H, et al. CTG repeat instability and size variation timing in DNA repair-deficient mice. The EMBO journal. 2003;22(9):2264-73.
37. Foiry L, Dong L, Savouret C, Hubert L, te Riele H, Junien C, et al. Msh3 is a limiting factor in the formation of intergenerational CTG expansions in DM1 transgenic mice. Human genetics. 2006;119(5):520-6.
38. Gomes-Pereira M, Fortune MT, Ingram L, McAbney JP, Monckton DG. Pms2 is a genetic enhancer of trinucleotide CAG.CTG repeat somatic mosaicism: implications for the mechanism of triplet repeat expansion. Human molecular genetics. 2004;13(16):1815-25.
39. Savouret C, Garcia-Cordier C, Megret J, te Riele H, Junien C, Gourdon G. MSH2-dependent germinal CTG repeat expansions are produced continuously in spermatogonia from DM1 transgenic mice. Molecular and cellular biology. 2004;24(2):629-37.
40. Lang WH, Coats JE, Majka J, Hura GL, Lin Y, Rasnik I, et al. Conformational trapping of mismatch recognition complex MSH2/MSH3 on repair-resistant DNA loops. Proceedings of the National Academy of Sciences of the United States of America. 2011;108(42):E837-44.
41. Zhao XN, Usdin K. The Repeat Expansion Diseases: The dark side of DNA repair. DNA repair. 2015;32:96-105.
42. Toscano A, Messina S, Campo GM, Di Leo R, Musumeci O, Rodolico C, et al. Oxidative stress in myotonic dystrophy type 1. Free radical research. 2005;39(7):771-6.
43. Ihara Y, Mori A, Hayabara T, Namba R, Nobukuni K, Sato K, et al. Free radicals, lipid peroxides and antioxidants in blood of patients with myotonic dystrophy. Journal of neurology. 1995;242(3):119-22.
44. Liu Y, Wilson SH. DNA base excision repair: a mechanism of trinucleotide repeat expansion. Trends in biochemical sciences. 2012;37(4):162-72.
45. Kovtun IV, Liu Y, Bjoras M, Klungland A, Wilson SH, McMurray CT. OGG1 initiates age-dependent CAG trinucleotide expansion in somatic cells. Nature. 2007;447(7143):447-52.
46. Seeberg E, Eide L, Bjoras M. The base excision repair pathway. Trends in biochemical sciences. 1995;20(10):391-7.

47. Lai Y, Budworth H, Beaver JM, Chan NL, Zhang Z, McMurray CT, et al. Crosstalk between MSH2-MSH3 and polbeta promotes trinucleotide repeat expansion during base excision repair. Nature communications. 2016;7:12465.
48. Goula AV, Merienne K. Abnormal base excision repair at trinucleotide repeats associated with diseases: a tissue-selective mechanism. Genes. 2013;4(3):375-87.
49. Jarem DA, Wilson NR, Delaney S. Structure-dependent DNA damage and repair in a trinucleotide repeat sequence. Biochemistry. 2009;48(28):6655-63.
50. de Souza-Pinto NC, Maynard S, Hashiguchi K, Hu J, Muftuoglu M, Bohr VA. The recombination protein RAD52 cooperates with the excision repair protein OGG1 for the repair of oxidative lesions in mammalian cells. Molecular and cellular biology. 2009;29(16):4441-54.
51. Kumar A, Kumar V, Singh SK, Muthuswamy S, Agarwal S. Imbalanced oxidant and antioxidant ratio in myotonic dystrophy type 1. Free radical research. 2014;48(4):503-10.
52. Marnett LJ. Oxyradicals and DNA damage. Carcinogenesis. 2000;21(3):361-70.
53. Stadtman ER, Levine RL. Protein oxidation. Annals of the New York Academy of Sciences. 2000;899:191-208.
54. Yla-Herttuala S. Oxidized LDL and atherogenesis. Annals of the New York Academy of Sciences. 1999;874:134-7.
55. Cadenas E, Davies KJ. Mitochondrial free radical generation, oxidative stress, and aging. Free radical biology & medicine. 2000;29(3-4):222-30.
56. Finkel T, Holbrook NJ. Oxidants, oxidative stress and the biology of ageing. Nature. 2000;408(6809):239-47.
57. Usuki F, Ishiura S. Expanded CTG repeats in myotonin protein kinase increase susceptibility to oxidative stress. Neuroreport. 1998;9(10):2291-6.
58. Usuki F, Takahashi N, Sasagawa N, Ishiura S. Differential signaling pathways following oxidative stress in mutant myotonin protein kinase cDNA-transfected C2C12 cell lines. Biochemical and biophysical research communications. 2000;267(3):739-43.
59. Bigot A, Klein AF, Gasnier E, Jacquemin V, Ravassard P, Butler-Browne G, et al. Large CTG repeats trigger p16-dependent premature senescence in myotonic dystrophy type 1 muscle precursor cells. The American journal of pathology. 2009;174(4):1435-42.

60. Furling D, Coiffier L, Mouly V, Barbet JP, St Guily JL, Taneja K, et al. Defective satellite cells in congenital myotonic dystrophy. Human molecular genetics. 2001;10(19):2079-87.
61. Blasco MA. Telomere length, stem cells and aging. Nature chemical biology. 2007;3(10):640-9.
62. de Lange T. Protection of mammalian telomeres. Oncogene. 2002;21(4):532-40.
63. de Lange T. Shelterin: the protein complex that shapes and safeguards human telomeres. Genes & development. 2005;19(18):2100-10.
64. de Lange T. How telomeres solve the end-protection problem. Science. 2009;326(5955):948-52.
65. Harley CB, Futcher AB, Greider CW. Telomeres shorten during ageing of human fibroblasts. Nature. 1990;345(6274):458-60.
66. Olovnikov AM. [Principle of marginotomy in template synthesis of polynucleotides]. Doklady Akademii nauk SSSR. 1971;201(6):1496-9.
67. Vaziri H, West MD, Allsopp RC, Davison TS, Wu YS, Arrowsmith CH, et al. ATM-dependent telomere loss in aging human diploid fibroblasts and DNA damage lead to the post-translational activation of p53 protein involving poly(ADP-ribose) polymerase. The EMBO journal. 1997;16(19):6018-33.
68. Bodnar AG, Ouellette M, Frolkis M, Holt SE, Chiu CP, Morin GB, et al. Extension of life-span by introduction of telomerase into normal human cells. Science. 1998;279(5349):349-52.
69. Di Donna S, Mamchaoui K, Cooper RN, Seigneurin-Venin S, Tremblay J, Butler-Browne GS, et al. Telomerase can extend the proliferative capacity of human myoblasts, but does not lead to their immortalization. Molecular cancer research : MCR. 2003;1(9):643-53.
70. Ramirez RD, Herbert BS, Vaughan MB, Zou Y, Gandia K, Morales CP, et al. Bypass of telomere-dependent replicative senescence (M1) upon overexpression of Cdk4 in normal human epithelial cells. Oncogene. 2003;22(3):433-44.
71. Zhu CH, Mouly V, Cooper RN, Mamchaoui K, Bigot A, Shay JW, et al. Cellular senescence in human myoblasts is overcome by human telomerase reverse transcriptase and cyclin-dependent kinase 4: consequences in aging muscle and therapeutic strategies for muscular dystrophies. Aging cell. 2007;6(4):515-23.
72. Kim WY, Sharpless NE. The regulation of INK4/ARF in cancer and aging. Cell. 2006;127(2):265-75.

73. Jacobs JJ, de Lange T. Significant role for p16INK4a in p53-independent telomere-directed senescence. Current biology : CB. 2004;14(24):2302-8.
74. Campisi J, d'Adda di Fagagna F. Cellular senescence: when bad things happen to good cells. Nature reviews Molecular cell biology. 2007;8(9):729-40.
75. Thornell LE, Lindstom M, Renault V, Klein A, Mouly V, Ansved T, et al. Satellite cell dysfunction contributes to the progressive muscle atrophy in myotonic dystrophy type 1. Neuropathology and applied neurobiology. 2009;35(6):603-13.
76. Longhese MP. DNA damage response at functional and dysfunctional telomeres. Genes & development. 2008;22(2):125-40.
77. Coluzzi E, Colamartino M, Cozzi R, Leone S, Meneghini C, O'Callaghan N, et al. Oxidative stress induces persistent telomeric DNA damage responsible for nuclear morphology change in mammalian cells. PloS one. 2014;9(10):e110963.
78. Oikawa S, Kawanishi S. Site-specific DNA damage at GGG sequence by oxidative stress may accelerate telomere shortening. FEBS letters. 1999;453(3):365-8.
79. von Zglinicki T. Oxidative stress shortens telomeres. Trends in biochemical sciences. 2002;27(7):339-44.
80. Natarajan AT. Mechanisms for induction of mutations and chromosome alterations. Environmental health perspectives. 1993;101 Suppl 3:225-9.
81. Jackson SP. Sensing and repairing DNA double-strand breaks. Carcinogenesis. 2002;23(5):687-96.
82. Lindahl T. Instability and decay of the primary structure of DNA. Nature. 1993;362(6422):709-15.
83. Savage JR, Papworth DG. Some problems of sampling for chromosomal aberrations from synchronous populations. Journal of theoretical biology. 1975;54(2):129-52.
84. Obe G, Pfeiffer P, Savage JR, Johannes C, Goedecke W, Jeppesen P, et al. Chromosomal aberrations: formation, identification and distribution. Mutation research. 2002;504(1-2):17-36.
85. Schwartz JL, Jordan R. Selective elimination of human lymphoid cells with unstable chromosome aberrations by p53-dependent apoptosis. Carcinogenesis. 1997;18(1):201-5.
86. Fenech M, Crott JW. Micronuclei, nucleoplasmic bridges and nuclear buds induced in folic acid deficient human lymphocytes-

evidence for breakage-fusion-bridge cycles in the cytokinesis-block micronucleus assay. Mutation research. 2002;504(1-2):131-6.
87. Fenech M. The in vitro micronucleus technique. Mutation research. 2000;455(1-2):81-95.
88. Fenech M. Cytokinesis-block micronucleus cytome assay. Nature protocols. 2007;2(5):1084-104.
89. Gisselsson D. Classification of chromosome segregation errors in cancer. Chromosoma. 2008;117(6):511-9.
90. Schueler MG, Sullivan BA. Structural and functional dynamics of human centromeric chromatin. Annual review of genomics and human genetics. 2006;7:301-13.
91. Pampalona J, Soler D, Genesca A, Tusell L. Telomere dysfunction and chromosome structure modulate the contribution of individual chromosomes in abnormal nuclear morphologies. Mutation research. 2010;683(1-2):16-22.
92. Murnane JP. Telomeres and chromosome instability. DNA repair. 2006;5(9-10):1082-92.
93. Thomas P, Umegaki K, Fenech M. Nucleoplasmic bridges are a sensitive measure of chromosome rearrangement in the cytokinesis-block micronucleus assay. Mutagenesis. 2003;18(2):187-94.
94. Vodenicharov MD, Wellinger RJ. DNA degradation at unprotected telomeres in yeast is regulated by the CDK1 (Cdc28/Clb) cell-cycle kinase. Molecular cell. 2006;24(1):127-37.
95. Holzmann K, Blin N, Welter C, Zang KD, Seitz G, Henn W. Telomeric associations and loss of telomeric DNA repeats in renal tumors. Genes, chromosomes & cancer. 1993;6(3):178-81.
96. Scandalios JG. Oxidative stress: molecular perception and transduction of signals triggering antioxidant gene defenses. Brazilian journal of medical and biological research = Revista brasileira de pesquisas medicas e biologicas. 2005;38(7):995-1014.
97. Petersen S, Saretzki G, von Zglinicki T. Preferential accumulation of single-stranded regions in telomeres of human fibroblasts. Experimental cell research. 1998;239(1):152-60.
98. Halliwell B, Aruoma OI. DNA damage by oxygen-derived species. Its mechanism and measurement in mammalian systems. FEBS letters. 1991;281(1-2):9-19.
99. Kaneko T, Tahara S, Taguchi T, Kondo H. Accumulation of oxidative DNA damage, 8-oxo-2'-deoxyguanosine, and change of

repair systems during in vitro cellular aging of cultured human skin fibroblasts. Mutation research. 2001;487(1-2):19-30.
100. Dodson ML, Lloyd RS. Mechanistic comparisons among base excision repair glycosylases. Free radical biology & medicine. 2002;32(8):678-82.
101. Grollman AP, Moriya M. Mutagenesis by 8-oxoguanine: an enemy within. Trends in genetics : TIG. 1993;9(7):246-9.
102. Memisoglu A, Samson L. Base excision repair in yeast and mammals. Mutation research. 2000;451(1-2):39-51.
103. Robertson AB, Klungland A, Rognes T, Leiros I. DNA repair in mammalian cells: Base excision repair: the long and short of it. Cellular and molecular life sciences : CMLS. 2009;66(6):981-93.
104. Hoeijmakers JH. DNA damage, aging, and cancer. The New England journal of medicine. 2009;361(15):1475-85.
105. Hussain SP, Hofseth LJ, Harris CC. Radical causes of cancer. Nature reviews Cancer. 2003;3(4):276-85.
106. Serra V, Grune T, Sitte N, Saretzki G, von Zglinicki T. Telomere length as a marker of oxidative stress in primary human fibroblast cultures. Annals of the New York Academy of Sciences. 2000;908:327-30.
107. von Zglinicki T, Pilger R, Sitte N. Accumulation of single-strand breaks is the major cause of telomere shortening in human fibroblasts. Free radical biology & medicine. 2000;28(1):64-74.
108. Saito M, Hisatome I, Nakajima S, Sato R. Possible mechanism of oxygen radical production by human eosinophils mediated by K+ channel activation. European journal of pharmacology. 1995;291(2):217-9.
109. Rhee DB, Ghosh A, Lu J, Bohr VA, Liu Y. Factors that influence telomeric oxidative base damage and repair by DNA glycosylase OGG1. DNA repair. 2011;10(1):34-44.
110. Opresko PL, Fan J, Danzy S, Wilson DM, 3rd, Bohr VA. Oxidative damage in telomeric DNA disrupts recognition by TRF1 and TRF2. Nucleic acids research. 2005;33(4):1230-9.
111. Wang Z, Rhee DB, Lu J, Bohr CT, Zhou F, Vallabhaneni H, et al. Characterization of oxidative guanine damage and repair in mammalian telomeres. PLoS genetics. 2010;6(5):e1000951.
112. Jackson SP. The DNA-damage response: new molecular insights and new approaches to cancer therapy. Biochemical Society transactions. 2009;37(Pt 3):483-94.

113. Dimitrova N, Chen YC, Spector DL, de Lange T. 53BP1 promotes non-homologous end joining of telomeres by increasing chromatin mobility. Nature. 2008;456(7221):524-8.
114. Ryan EL, Hollingworth R, Grand RJ. Activation of the DNA Damage Response by RNA Viruses. Biomolecules. 2016;6(1):2.
115. Takai H, Smogorzewska A, de Lange T. DNA damage foci at dysfunctional telomeres. Current biology : CB. 2003;13(17):1549-56.
116. Kamsteeg EJ, Kress W, Catalli C, Hertz JM, Witsch-Baumgartner M, Buckley MF, et al. Best practice guidelines and recommendations on the molecular diagnosis of myotonic dystrophy types 1 and 2. European journal of human genetics : EJHG. 2012;20(12):1203-8.
117. Dimri GP, Lee X, Basile G, Acosta M, Scott G, Roskelley C, et al. A biomarker that identifies senescent human cells in culture and in aging skin in vivo. Proceedings of the National Academy of Sciences of the United States of America. 1995;92(20):9363-7.
118. Fortini P, Pascucci B, Parlanti E, D'Errico M, Simonelli V, Dogliotti E. 8-Oxoguanine DNA damage: at the crossroad of alternative repair pathways. Mutation research. 2003;531(1-2):127-39.
119. Russo MT, De Luca G, Degan P, Bignami M. Different DNA repair strategies to combat the threat from 8-oxoguanine. Mutation research. 2007;614(1-2):69-76.
120. Warner JP, Barron LH, Goudie D, Kelly K, Dow D, Fitzpatrick DR, et al. A general method for the detection of large CAG repeat expansions by fluorescent PCR. Journal of medical genetics. 1996;33(12):1022-6.
121. Musova Z, Mazanec R, Krepelova A, Ehler E, Vales J, Jaklova R, et al. Highly unstable sequence interruptions of the CTG repeat in the myotonic dystrophy gene. American journal of medical genetics Part A. 2009;149A(7):1365-74.
122. Radvansky J, Ficek A, Minarik G, Palffy R, Kadasi L. Effect of unexpected sequence interruptions to conventional PCR and repeat primed PCR in myotonic dystrophy type 1 testing. Diagnostic molecular pathology : the American journal of surgical pathology, part B. 2011;20(1):48-51.
123. Gennarelli M, Pavoni M, Amicucci P, Novelli G, Dallapiccola B. A single polymerase chain reaction-based protocol for detecting normal and expanded alleles in myotonic dystrophy. Diagnostic molecular pathology : the American journal of surgical pathology, part B. 1998;7(3):135-7.

124. Durante M, Furusawa Y, Gotoh E. A simple method for simultaneous interphase-metaphase chromosome analysis in biodosimetry. International journal of radiation biology. 1998;74(4):457-62.
125. Speicher MR, Gwyn Ballard S, Ward DC. Karyotyping human chromosomes by combinatorial multi-fluor FISH. Nature genetics. 1996;12(4):368-75.
126. Cornforth MN. Analyzing radiation-induced complex chromosome rearrangements by combinatorial painting. Radiation research. 2001;155(5):643-59.
127. Festa F, Cristaldi M, Ieradi LA, Moreno S, Cozzi R. The Comet assay for the detection of DNA damage in Mus spretus from Donana National Park. Environmental research. 2003;91(1):54-61.
128. Collins AR, Duthie SJ, Dobson VL. Direct enzymic detection of endogenous oxidative base damage in human lymphocyte DNA. Carcinogenesis. 1993;14(9):1733-5.
129. Collins AR. The comet assay for DNA damage and repair: principles, applications, and limitations. Molecular biotechnology. 2004;26(3):249-61.
130. Kirsch-Volders M, Tallon I, Tanzarella C, Sgura A, Hermine T, Parry EM, et al. Mitotic non-disjunction as a mechanism for in vitro aneuploidy induction by X-rays in primary human cells. Mutagenesis. 1996;11(4):307-13.
131. Slijepcevic P. Telomere length measurement by Q-FISH. Methods in cell science : an official journal of the Society for In Vitro Biology. 2001;23(1-3):17-22.
132. Perner S, Bruderlein S, Hasel C, Waibel I, Holdenried A, Ciloglu N, et al. Quantifying telomere lengths of human individual chromosome arms by centromere-calibrated fluorescence in situ hybridization and digital imaging. The American journal of pathology. 2003;163(5):1751-6.
133. Berardinelli F, Antoccia A, Buonsante R, Gerardi S, Cherubini R, De Nadal V, et al. The role of telomere length modulation in delayed chromosome instability induced by ionizing radiation in human primary fibroblasts. Environmental and molecular mutagenesis. 2013;54(3):172-9.
134. Wong HP, Slijepcevic P. Telomere length measurement in mouse chromosomes by a modified Q-FISH method. Cytogenetic and genome research. 2004;105(2-4):464-70.

9. MATERIALS AND METHODS

Cell and culture conditions

Human primary fibroblasts derived from skin biopsies of DM1 patients and healthy people (WT) (University of Roma Tor Vergata), were grown in Dulbecco's modified Eagle's medium (DMEM) (Euroclone, Italy) supplemented with 10% inactivated foetal bovine serum (Euroclone, Italy), 10,000 units/ml penicillin and streptomycin 10mg/ml (Biological Industries, Israel), 1% L-Glutamine, 1% sodium pyruvate (Euroclone, Italy) and 1% non-essential amminoacids (Euroclone, Italy), at 37°C in 95% air and 5% CO_2 incubator.

PCR and fragment-length analysis

In the lower range of DM1 expansions, the best analytical method is PCR. Alleles containing between 5 and 100 to 125 CTG-repeat units can be detected and characterized using synthetic fluorescently-labelled primers flanking the CTG-repeat region, followed by direct analysis of the length of the amplified products by capillary electrophoresis.

Primers used on DMPK gene (sequence 5'-3'):

Forward: CTCGAAGGGTCCTTGTAGCC

Reverse: TGCACAAGAAAGCTTTGCAC

Triplet-repeat Primed (TP)-PCR

After PCR and fragment-length analysis, DM1 and WT fibroblasts were subjected to TP-PCR. TP-PCR is a PCR with three primers, where one lies outside the repeat, one within the repeat (which is added in limiting amounts) that also has a sequence-tail complementary to the third, universal, and fluorescently-labelled primer (120). This will result in a mixture of PCR fragments of different sizes that can be analyzed by capillary electrophoresis. Although expansions in all size ranges can be detected by TP-PCR, no reliable information about the length of the expanded repeat will be obtained because of extinction of the signal in the higher size region. In DM1 expansion analysis, the TP-PCR has proven to be an accurate technique. Nevertheless, the presence of rare interruptions of the otherwise pure CTG repeat (121) may result in aberrant patterns or failure to detect expansions with TP-PCR (122). Therefore, to exclude false-negative reports, we performed long-range PCR in order to confirm the trinucleotide expansion size.

Primers used on DMPK gene (sequence 5'-3'):
Forward: GAAGGGTCCTTGTAGCCGGGAA
Reverse: ACGCATCCCAGTTTGAGACGCAGCAGCAGCAGCAG
Universal: TACGCATCCCAGTTTGAGACG

Southern blotting of long-range PCR-products
This Southern blot method requires precise PCR conditions to ensure the amplification of larger fragments, monitored by using appropriate positive and negative (healthy) controls, followed by probing with an end-labelled (CTG)x (where x is 5 or more) probe (123). On these Southern blots, expanded DMPK alleles will appear in virtually all cases as smears or multiple fragments, which is (in part) owing to somatic heterogeneity. In addition, as with the TP-PCR, interrupted repeats may remain undetectable under certain conditions.
Primers used on DMPK gene (sequence 5'-3'):
Forward: CCGTTGGAAGACTGAGTG
Reverse: CTGGCCGAAAGAAAGAAATG

TaqMan Real-time qPCR
Total RNA was extracted from DM1 and WT fibroblasts using TRIzol reagent (Invitrogen, California, USA), according to the manufacturer's instructions. The quality and quantity of RNA were assessed by using Nano Drop ND-1000 spectrophotometer (ThermoFisher Scientific, Massachusetts, USA). 500 ng of total RNA were transcribed into cDNA using High Capacity cDNA Reverse Transcription Kit (Applied Biosystem, California, USA). Then, for real-time qPCR, 30ng cDNA were added to TaqMan Gene Expression Master Mix 2X (Applied Biosystem, California, USA) and dispended in TaqMan Array 96-Well Fast Plates (Applied Biosystem, California, USA), specifically designed to analyze BER and MMR genes (Tab.4).
Thermal cycling conditions on 7500 Fast Real-Time PCR System (Applied Biosystem, California, USA) consisted of holding stage at 50 °C for 2 mins and 95 °C for 10 mins followed by 40 cycles of each PCR step: (denaturation) 95 °C for 15 secs and (annealing/extension) 60 °C for 1 min. The relative fold-change $2^{-\Delta\Delta CT}$ method was used to determine the relative quantitative gene expression compared with *PPIA* (Hs04194521_s1) as endogenous controls. Data were expressed as the mean ± standard deviation (SD).

Table 4 Genes analized in TaqMan Real-Time qPCR

Assay ID	Gene Symbol(s)
Hs99999901_s1	18s rRNA
Hs04194521_s1	PPIA
Hs02786624_g1	GAPDH
Hs00172396_m1	APEX1
Hs00213454_m1	OGG1
Hs01099715_m1	POLB
Hs00242692_m1	LIG3
Hs00427214_g1	PCNA
Hs00953527_m1	MSH2
Hs00989003_m1	MSH3
Hs00943000_m1	MSH6
Hs00979919_m1	MLH1
Hs00998142_m1	MLH3
Hs00922262_m1	PMS1
Hs00241053_m1	PMS2

Irradiation Procedure

For X-ray irradiation, cells were seeded on plates at least 48 hrs before treatment at the density of 3 x 10^5 cells per culture flask and irradiated at room temperature (RT) using a Gilardoni apparatus (250 kV, 6 mA, dose-rate 0.53 Gy/min). Unless otherwise indicated cells were irradiated with a dose of 2 Gy and cells not irradiated were used as control in all the experiments.

Collection of chromosome spreads

After treatment, PBS washed out media and cells were trypsinized and sown at the density of 3 x 10^5 cells per culture flask and left to grow in complete medium and collected at different experimental points.
Chromosome spreads were obtained following 30 mins incubation in 50 µM calyculin-A (Wako, Germany), (124). Spreads of these prematurely condensed chromosomes (PCC) were prepared by a

standard procedure consisting of treatment with a hypotonic solution (75 mM KCl) for 28 mins at 37°C, followed by fixation in freshly prepared Carnoy solution (3:1 v/v methanol/acetic acid). Cells were then dropped onto slides, air dried, and utilized for cytogenetic analysis.

Multicolor-Fluorescence "in situ" Hybridization Analysis (M-FISH)

Multicolor-fish (125) is a cytogenetic molecular technique very useful not only for the identification of biomarkers for densely ionizing radiation exposure, but also for analyzing in detail several aspects of the nature of chromosome aberrations, such as the distribution among chromosomal regions, the dependence on the dose and the quality of radiation.

Fixed cells were dropped onto glass slides and hybridized with the 24XCytenHuman Multicolor FISH Probe kit (MetaSystems, Germany), following the manufacturer's instruction. The slides were denatured in 0.07N NaOH and then rinsed in a graded ethanol series. Meanwhile, the probe mix was denatured using a MJ mini personal thermal cycler (Bio-Rad laboratories, California, USA) with the following program: 5 mins at 75 °C, 30 secs at 10 °C, and 30 mins at 37 °C. The probes were added to the slides and a coverslip was added and sealed using rubber cement. The samples were then hybridized in a humidified chamber at 37 °C for 48 hrs, washed in saline-sodium citrate (SSC) buffer for 5 mins at 75 °C and counterstained with DAPI. Finally, metaphases were visualized and captured using an Axio-Imager M1 microscope (Zeiss, Germany) equipped with a coupled charged device (CCD) camera. The karyotyping and cytogenetic analysis of each single chromosome was performed using the ISIS software (MetaSystems, Germany). Each chromosome of a metaphase spread was examined based on its unique fluorochrome profile. Structural chromosome aberrations were classified following the mPAINT system (126). The aberrations were scored as chromosome breaks, acentric fragments (i.e., fragments that were not associated with an exchange) and chromosome exchanges (translocations). Experiments were repeated at least two times, and the mFISH analysis was performed using at least 100 metaphase spreads for each irradiated and not irradiated control samples.

H_2O_2 treatment

Cells were sown on plates 48 hrs before treatment at the density of 3 x 10^5 cells per culture flask. Subconfluent cells were treated with H_2O_2 (10vol-3%), in a complete medium, at the final concentration of 200 μM for 1 hr at 37°C in 95% air and 5% CO_2 incubator. Cells examined after treatment with H_2O_2 were compared to parallel cultured control cells grown in the medium without H_2O_2.

Standard and FPG-modified alkaline comet assay

DM1 and WT cells were analyzed by alkaline comet assay as described by Festa et al. (127) to verify the DNA damage induced by H_2O_2 treatment. After 1 hr treatment, cells were immediately subjected to the assay (time 0) or grown in fresh medium for different recovery times (5 and 24 hrs) to evaluate the activation of repair pathways over time and then subjected to the alkaline comet assay. After trypsinization, all samples were incubated for 30 mins at 37°C in 95% air and 5% CO_2 incubator. At the end of treatment, before performing comet assay, an aliquot of cells from each sample was dyed with trypan blue (Sigma- Aldrich, Missouri, USA) in order to evaluate the percentage of cell death (blue stained cells). This percentage never exceeded 10% in all experimental conditions.

The assay was performed using a FPG FLARE module kit (Trevigen, Gaithersburg, MD). We used formamidopyrimidine-DNA-glycosylase (FPG)-modified comet assay to evaluate oxidative DNA damage. FPG is a glycolase that recognizes and specifically cuts the oxidized bases principally 8-oxoG from DNA, producing apurinic sites converted in breaks by the associated AP-endonuclease activity. Therefore, these breaks can be detected by comet assay and give a measure of oxidative DNA damage, enabling us to detect moderate, but still appreciable damage. We followed the procedure described by Collins et al. (128), with minor modifications. Within the module, the manufacturer provided all the reagents used. Slides were analyzed using a fluorescence microscope (Leica, Germany) equipped with a camera. Seventy comets on each slide of 2 independent experiments, were acquired using "I.A.S." software automatic image analysis system purchased from Delta Sistemi (Rome-Italy). To quantify the induced DNA damage we used the Tail DNA (TD%), which is a measure of the percentage of migrated DNA in the tail (129).

SyBR Green Real-time qPCR

To confirm the expression levels of genes resulted statistically significant, a SYBR Green qPCR assay was performed. Total RNA was extracted from DM1 and WT fibroblasts at 2 different experimental times (45 mins of treatment and 3 hrs after 1 hr of treatment) using TRIzol reagent (Invitrogen, California, USA), according to the manufacturer's instructions. The quality and quantity of RNA were assessed by using Nano Drop ND-1000 spectrophotometer (ThermoFisher Scientific, Massachusetts, USA). 500 ng of total RNA were transcribed into cDNA using High Capacity cDNA Reverse Transcription Kit (Applied Biosystem, California, USA). Specific primers were designed and validated to verify their efficiency. The qPCR assay was performed adding the cDNA in reaction mix containing a final concentration of 1X Power SYBR Green PCR Master Mix (Applied Biosystem, California, USA) and 0.3 μM of primers. The amplification and detection were performed in 7500 Fast Real-Time PCR System (Applied Biosystem, California, USA), using the following thermal cycling condition: 95 °C (10 mins), then 40 cycles of 95 °C (15 secs), 61 °C (1 min). Each quantification was done in duplicate for every sample. Relative expression levels were calculated using the $2^{-\Delta\Delta CT}$ method and PPIA level expression was used as reference gene. The primers used are:

OGG1 Forward: GGCTCAGAAATTCCAAGGTG
OGG1 Reverse: GGCGATGTTGTTGTTGGAG
POLBForward: TGCCCTAGAAAAGGGTTTCAC
POLB Reverse: TTCTCCTGCAACTCCAGTGAC
PCNAForward: CACTAAGGGCCGAAGATAACG
PCNA Reverse: GAAACTTTCTCCTGGTTTGGTG
MLH1 Forward: AGCAGGGACATGAGGTTCTC
MLH1 Reverse: CCACTGAGGATTCACACAGC
PMS1 Forward: TGAATGTAGACCTCGCAAAGTG
PMS1 Reverse: TGGGTAATTGTCTGGATAGACG
PPIAForward: TCTGCGTGAATTACCACCAC
PPIA Reverse: ATTTCCACCTTGCACTCAGG

Cytokinesis-block micronucleus assay

After 1 hr; 200 μM H_2O_2 treatment cells were plated on petri dish at different density and Bi-nucleated (BN) DM1 and WT were obtained adding Cytocalasin B (1mg/ml stock solution in dimethyl sulphoxide; Sigma Aldrich, Missouri, USA) at a final concentration of 3 μg/ml 24 hrs before fixation at 48 and 72 hrs (130). The culture was fixed in freshly prepared modified Carnoy solution (5:1 v/v methanol/acetic acid) and afterward dyed with DAPI (Sigma Aldrich, Missouri, USA) in Vectashield (Vector Laboratories, California, USA). The analysis of abnormal nuclear morphologies was performed on 1000 BN cells. Experiments were repeated at least two times.

Abnormal Nuclear Morphologies (ANMs) scoring criteria

BN cells were scored as previously described by Fenech, (87). Briefly, daughter nuclei must be situated in the same cytoplasm, had approximately the same size, staining pattern and staining intensity. MN was considered as a small nucleus, morphologically identical to the cell nucleus. NBUD was considered a small nucleus but connected to the cell nucleus. NPB was considered to be the DNA connection between the two daughter nuclei (86).

Quantitative-Fluorescence "in situ" Hybridization Analysis (Q-FISH)

The Q-FISH technique was based on the use of peptide nucleic acid (PNA) telomere oligonucleotides that generate stronger and more specific hybridization signals than the same DNA oligonucleotides. The resolution of Q-FISH was in the region of about 200 bp (131). The Q-FISH allowed: (i) precise measurement of individual telomeres at every single chromosome arm (ii) to detect even small differences in telomere length (132). Q-FISH staining was performed as previously described by Berardinelli et al. (133) with minor modifications. Briefly slides and probes (Cy3 linked telomeric, PANAGENE, Korea and chromosome 2 centromeric Peptide Nucleic Acid PNA probes DAKO Cytomatation, Denmark) were co-denatured at 80°C for 3 mins and hybridized for 2 hrs at RT in a humidified chamber. Slides were counterstained with 4,6-diamidino-2 phenylindole (DAPI, Sigma Aldrich, Missouri, USA) in Vectashield (Vector Laboratories, California, USA). Q-FISH technique required appropriate digital image analysis system designed to control acquisition of digital images, as well as to perform fluorescence

intensity measurement (131). However, Q-FISH is a complex technique and it requires proper calibration protocols to eliminate inherent variations associated with fluorescence microscopy (134). In our laboratory, we use centromere of chromosomes 2 as the internal reference in each metaphase analyzed. Images were captured at a 63X magnification with an Axio Imager M1 (Zeiss, Germany) equipped with a coupled charged device (CCD) camera. The telomere size was analyzed with ISIS software (MetaSystems, Germany). In particular the software calculates telomere lengths as the ratio between the total telomeres fluorescence (T) and the fluorescence of the centromere of the two chromosomes 2 (C). Data were expressed as a percentage (T/C%) (132). Experiments were repeated at least two times, and at least 10 metaphases were scored for each experiment.

Co-immunofluorescence

After 1 hr treatment with 200 μM H_2O_2, cells were trypsinized and seeded on a glass in a petri dish. After 48 hrs from treatment, the slides were fixed with 4% paraformaldehyde (Sigma Aldrich, Missouri, USA), permeabilized in 0.2% Triton X-100 and blocked in PBS/BSA 1% for 30 mins at RT. Slides were incubated with a mouse mono-clonal anti-phospho-histone H2AX antibody (Millipore, California, USA) and a rabbit poly-clonal-TRF1 antibody (Santa Cruz Biotechnology, Texas, USA) overnight at 4°C, washed in PBS/BSA 1% and then exposed to the secondary Alexa Fluor 546-labelled goat anti-mouse antibody (Invitrogen, Life Technologies, California, USA) for H2AX and Alexa Fluor 488 labelled goat anti-rabbit (Invitrogen, Life Technologies, California, USA) for TRF1, for 1 hr at 37°C. After washes in PBS/BSA 1% DNA was counterstained by DAPI (Sigma Aldrich, Missouri, USA) in Vectashield (Vector Laboratories, California, USA). Cells were analyzed with fluorescence microscopy using an Axio Imager M1 microscope (Zeiss, Germany) equipped with a CCD camera. The frequency of foci per cell and TIF per cell were scored in 100 nuclei in at least two independent experiments.

Growth rate analysis

After H_2O_2 treatment cells were seeded at the density of 10^5 cells; every 24 hrs cells were detached and counted with a Burker's chamber (Sigma Aldrich, Missouri, USA) up to 168 hrs.

The total amount of cells in our samples was calculated as follows:

Total cells = (mean of cells number per A-square) x 10^4 x total volume (mL)

The percentage of viable cells was detected after having incubated cells with Trypan blue (Sigma- Aldrich, Missouri, USA) for 3 mins. The experiment was repeated at least two times.

Senescence beta-galactosidase Staining

To test if H_2O_2 treatment induces premature senescence in our samples, after 1 hr (200 μM) H_2O_2 treatment cells were plated on petri dish at different density to be fixed after 48 and 96 hrs and stained using Senescence beta-galactosidase Staining kit (Cell signaling technology, Massachusetts, USA). β-galactosidase is in fact a hydrolyze enzyme that catalyzes the hydrolysis of β-galactoside into monosaccharides only in senescent cells (117)**.** Briefly, cells were washed one time with 1X PBS and then was added 1 ml of 1X Fixative Solution for 10-15 mins at RT. After two washes in 1X PBS, 1 ml of the β-Galactosidase Staining Solution was added to each well. Petri dishes were incubated at 37°C overnight in a dry incubator. While the β-galactosidase was still on the plate, the cells were checked under a microscope (200X total magnification) for the development of blue color. At least 100 cells were counted in two independent experiments and the frequency of blu/total cells were scored.

Data analysis

We used the student's t-test for the statistical analysis for all our data. Significance was accepted for value $p<0.05$.